Physics Department-University of Crete

IESL-FORTH

“Preparation of polarized atoms via the hyperfine interaction”

Sofikitis Dimitris

Supervisor: T. Peter Rakitzis

Heraklion

2006

(A) INTRODUCTION

In recent decades, control over spin and, more generally, over quantum angular momentum has led to many technological advances, such as NMR and medical imaging [1,2], and has allowed the study of many spin-dependent phenomena, such as nuclear, atomic, molecular and surface scattering [3,4,5]. Angular momentum polarization also plays a very important role in chemical dynamics, as the spatial direction of the angular momentum of the different species involved in a chemical reaction plays a fundamental role in the way the interaction takes place [6,7].

There exist several methods for the preparation of spin polarized gases (atomic or molecular). These methods include Stern-Gerlach separation[8,9], optical pumping and spin-exchange optical pumping[10,12,13] and lately molecular photodissociation with circularly polarized light[14,17,18,19]. Each of these techniques has specific limits concerning the maximum degree of polarization and the density of the polarized gas that can be achieved and the repetition rate in which they can operate. As the utilities of spin polarized gasses move from scientific research towards technological application, the need to reach higher densities and higher preparation repetition rates becomes evident. We will outline these methods in the following, in order to point out the fundamental reasons for which, application of these techniques to several technological areas is restricted. This review will be also helpful to point out the initiative for developing the technique described here, which is preparing polarized gases via polarization transfer from molecular rotation to the nuclear spin.

1 Existing methods for the preparation of spin polarized molecules and atoms.

a) Stern-Gerlach separation.

Spin-polarized atoms were first produced using the Stern-Gerlach separation technique [8,9]. This technique, exploits the fact that a charged particle's angular momentum interacts directly with the gradient of the magnetic field. Thus, when an atomic beam is passed through a magnetic field which has non zero gradient in one specific direction z the force acting in the charged particle is proportional to the particle's angular momentum projection in that direction.

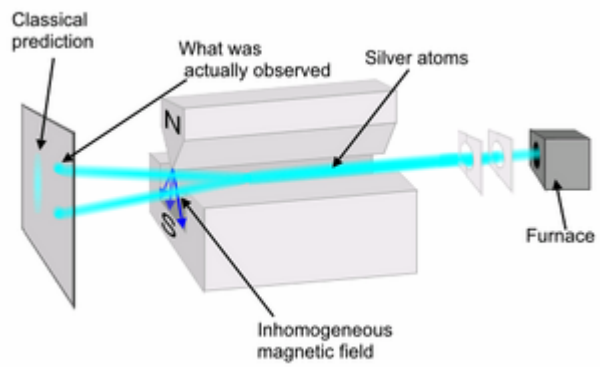

Figure 1: The basic elements of the Stern-Gerlach separation technique.

The basic elements of the Stern-Gerlach experiment are used for the preparation of spin polarized gases via the technique known as Stern-Gerlach separation. This technique remains the most general method for producing polarized atoms, as long as an appropriate atomic beam can be produced. Drawbacks include the complexity of the experimental setup, the limited atomic beam density (of about 10^{14} atoms/s in favorable cases), and the poor time-resolution.

b) Optical pumping and Spin Exchange Optical pumping (SEOP).

Optical pumping [10] is a very powerful technique, and variants of optical pumping are used in various fields of modern atomic physics, such as laser cooling, Bose-Einstein condensation, and the production of spin polarized atoms. A typical optical pumping scheme is shown in Figure 1. Circular polarized light (σ(+) excitation shown here) pumps the m=-1/2 ground state of Rubidium to the m=+1/2 excited state, whereas the m=+1/2 ground state cannot be pumped as there is no m=+3/2 excited state. Collisional quenching transfers population back to both ground spin states. The m=+1/2 state has no significant losses, whereas it has significant gains from excited state quenching; therefore, after several absorption cycles, nearly 100% of the population is transferred to the m=+1/2 state. The hyperfine interaction transfers polarization to the nuclear spin, so that, after additional pumping, the nuclear spin is also polarized.

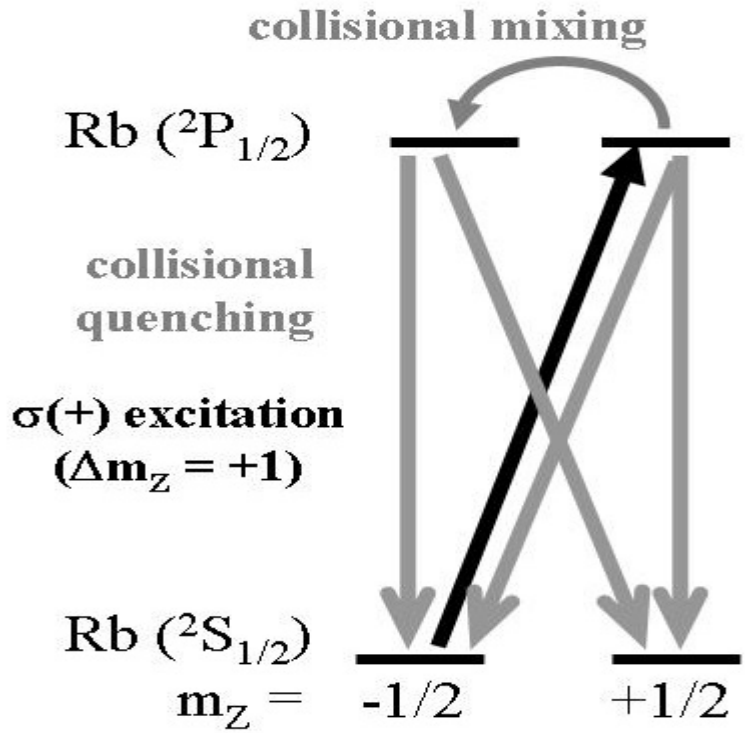

Figure 2: Optical pumping scheme for Rb for σ(+) excitation, showing population transfer from the m=-1/2 ground state to the m=+1/2 state via optical excitation and collisional quenching.

The success of optical pumping hinges on a large pumping rate (compared to the depolarization rate). Optical pumping has proved extremely successful for the alkali atoms, which have very strong appropriate transitions (with absorption cross sections $\sigma_{abs} \approx 10^{-10}$ cm^2) in the visible where powerful cw laser sources are readily available. However, most other atoms do not have strong ground-state absorptions where powerful cw sources are currently available, and thus optical pumping has been limited to mostly the alkali atoms. Recently, a very weak cw source at Lyman-α was produced which may allow laser cooling of hydrogen atoms [11]. Improvements in this direction may make optical pumping applicable to other atoms. A further extension of the optical pumping technique is spin-exchange optical pumping (SEOP) [12,13]. Noble gases with non-zero nuclear spin (e.g. ^{3}He and ^{129}Xe) are mixed with alkali atoms as they are optically pumped. For example, Rubidium electronic spin-polarization is transferred to the ^{3}He nuclear spin via collisions:

$$\mathrm{Rb}(\uparrow e) + {}^3\mathrm{He}\,(\downarrow n) \rightarrow \mathrm{Rb}(\downarrow e) + {}^3\mathrm{He}\,(\uparrow n) \qquad (1)$$

Using this technique, several atmospheres of ^{3}He can be polarized to P=70% over several hours of SEOP.

Polarized noble gasses find direct application in medical imaging. Those gasses can be inhaled and since their polarization can be remotely detected (with superconducting or any other type of magnetometer), the lung airways can be visualized.

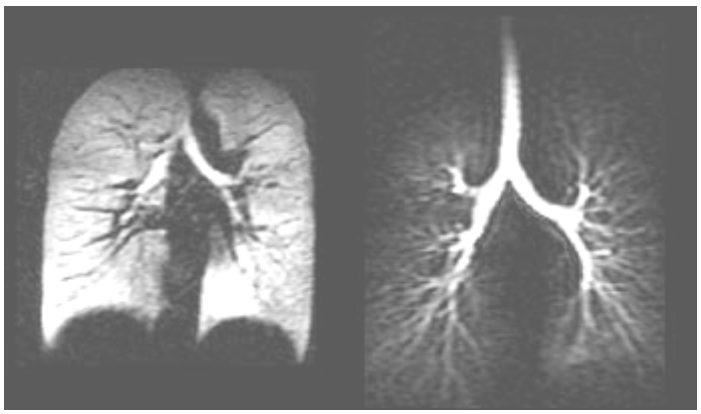

Figure 3: Imaging the lung with helium polarized via SEOP.

c) Preparation of polarized atoms from molecular photodissociation.

A method for producing high-density polarized atoms from the photodissociation of diatomic molecules was proposed by van Brunt and Zare in 1968 [14], which exploits the fact that the projection of electronic angular momentum, for prompt photodissociation, is conserved within the atomic photofragments. In fact, the electronic states of diatomic molecules correlate adiabatically, at large internuclear separation, to atoms in specific |JM> states:

$$AB(\Omega_i) \xrightarrow{R\to\infty} A(J_A,M_A) + B(J_B,M_B) \qquad (2)$$

where AB is a diatomic molecule, Ω_i is the projection of the total electronic angular momentum of electronic state *i* along the AB bond axis, and (J_A,M_A) and (J_B,M_B) are the atomic states of atoms A and B, respectively. Conservation of angular momentum projection along the recoil direction yields the important constraint:

$$\Omega_i = M_A + M_B \qquad (3)$$

For optical excitation of a particular Ω_i state, prompt adiabatic dissociation will produce atoms in particular m states.

As an example let us consider the prompt photodissociation of HCl molecules with circularly polarized light.

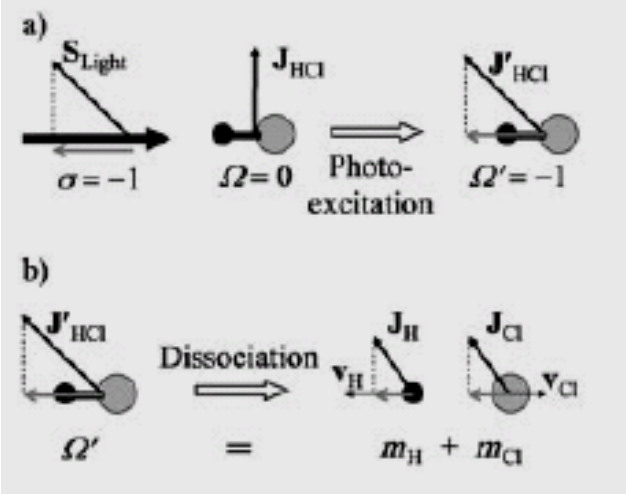

Figure 4: a) photoexcitation and b) dissociation of HCl with circularly polarized light.

The absorption of left circularly polarized light (s=-1) (propagating parallel to the HCl bond) by ground state HCl (Ω=0) produces excited state HCl with Ω=-1. In the dissociation step, the conservation of Ω between the atomic photofragment angular momentum projections m_H and m_{Cl} produces polarized atoms.

The strength of the idea is that the mechanism of production of the polarized atoms is a natural physical process (photodissociation) and does not require a complicated experimental preparation, such as Stern-Gerlach separation. In addition, the density of the polarized atoms can be extremely high, approximately as high as the parent molecule density, which is much higher than that possible with most other techniques. Possible disadvantages include: a) exclusive optical excitation of particular Ω_i states is not always possible, b) dissociation is not necessarily adiabatic, c) even for adiabatic dissociation the photofragment atomic polarization is not necessarily 100% and is often less, d) maximum polarization (in the case of atomic orientation) is achieved only for recoil directions parallel to the quantization axis of the photolysis laser (i.e. the propagation direction), whereas the polarization of photofragments recoiling at an angle θ will be reduced by cosθ and e) the electronic polarization of the atoms will be reduced by any nonzero nuclear spins due to hyperfine depolarization [15]. Experimental studies show that even in the presence of disadvantages a) b) and c) large degree of polarization can be achieved for many atoms in densities higher than the previous techniques, and experimental velocity resolution solves point d). The technique presented here can be used to overcome point e) while it can be used also as an independent technique for the preparation of polarized atoms.

The electronic polarization reduction due to the presence of unpolarized nuclear spin is caused by a quantum beating phenomena that is responsible for polarization exchange between the electron and the nuclear spin in a sub-nanosecond timescale. The nature of this quantum beating phenomena can be explored with the use of a simple model of a double, symmetric quantum well.

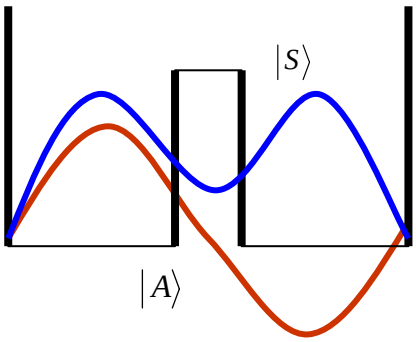

Figure 5: A symmetric double quantum well, with the two eigenfunctions that are solutions of the Schrödinger equation for this system: the symmetric and the anti-symmetric solution.

The Schrödinger equation for this system yields two eigenstates of slightly different energy, the symmetric and the anti-symmetric one. If now we consider a particle confined in the one side of the double well, it's wavefunction has to be written as a superposition of these two eigenstates and in particularly addition for the right side and difference for the left.

$$|R\rangle = \frac{1}{\sqrt{2}}\left(|S\rangle + |A\rangle\right)$$

$$|L\rangle = \frac{1}{\sqrt{2}}\left(|S\rangle - |A\rangle\right)$$

Since these quantum states are a superposition of eigenstates with different energy they exhibit time dependence. For example for the right state the time-dependence is such that if we extract a phase the superposition now contains a harmonic term in front of the anti-symmetric component.

$$|R\rangle \xrightarrow{Time} \frac{1}{\sqrt{2}}\left(e^{-\imath E_S t/\hbar}|S\rangle + e^{-\imath E_A t/\hbar}|A\rangle\right) = \frac{e^{-\imath E_S t/\hbar}}{\sqrt{2}}\left(|S\rangle + e^{-\imath (E_A - E_S)t/\hbar}|A\rangle\right)$$

After the time equal to $t = \pi\hbar/\Delta E$, this harmonic term will change the sign in the superposition changing the state from right to left. After twice that time the state is again right and this flipping continues harmonically. Thus if we confine the particle in one side of the quantum well, it will be bouncing form right to left in a periodic fashion.

The same situation occurs if we prepare an atom with it's electron spin **S** polarized and it's nuclear spin **I** unpolarized. Those two angular momentum entities are coupled to form the total angular momentum state **F** which is the "good" quantum number of the system. The following picture shows the situation for **S** = **I** = ½.

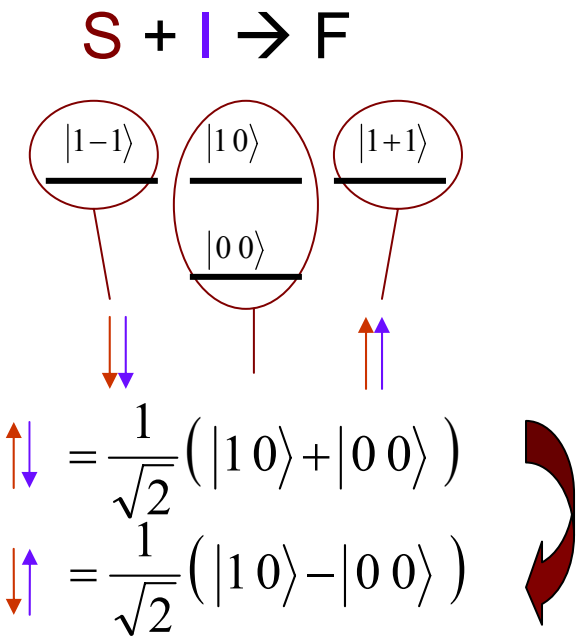

Figure 6: Total angular momentum states for an atom with S = I = ½. The co-oriented spins correspond to eigenstates of the system while the counter – oriented to superposition of total angular momentum states.

As we see in the figure, the co-oriented spins are eigenstates of the system while the counter – oriented are superpositions of them. Thus if the system is found in one of the counter – oriented spin states, it will be found in the other at later times and this situation will continue in a harmonic way.

When a technique can produce a collection of atoms with their electron spin totally oriented but with the nuclear spin unpolarized, it actually puts half of the atomic population in one of the co-oriented, time-independent spin states and the other half in one of the two counter-oriented, time-dependent spin states. Changing from one counter-oriented spin states to the other causes the total polarization to bounce from the electronic to the nuclear spin in sub-nanosecond timescales.

The method proposed here aims in overcoming this problem by making use of a similar depolarization effect observed when optical methods are employed to polarize a molecule's rotational angular momentum. The molecular rotation is similarly

coupled to the nuclear spin and polarization is transferred from the molecular rotation to the nuclear spin and back, only in much shorter timescales (in the order of μs). Photodissociation of the molecule in appropriate times leads to the production of atoms with their nuclear spin polarized.

2 Preparation of polarized atoms via polarization transfer from molecular rotation to the nuclear spin.

The use of optical methods for the preparation of aligned or oriented reagents in physical chemistry led to the observation of polarization transfer from the molecular rotation to the nuclear spin[16,17,18]. In experiments where optically prepared reagents where used for studies of reaction dynamics, the depolarization exhibited in microsecond timescales had to be explained, so that its effect in the experimental results is quantified. This depolarization was attributed to the presence of the nuclear spin [19] an explanation that led to predictions verified by the experimental measurements for many molecular systems [15,20].

Molecules and atoms in general, contain more than one angular momentum entity. These can be the angular momentum associated with molecular rotation or the, often symbolized as J, the electronic angular momentum L and intrinsic angular momentum (spin) S and finally the nuclear spin I. The angular momentum entities associated with the electron are usually weakly coupled to the ones associated to the nuclei via the hyperfine interaction, thus they are considered to be independent from each other in relatively short timescales. In optical excitation of molecules (where the process is done with no hyperfine resolution), the absorption process tends to align (or orient depending in the light being linearly or circularly polarized) the angular momentum J leaving unaffected the nuclear spin I that the molecule possesses. This is a consequence of the weak coupling of these spins and the short duration of the excitation process compared to the precision rates of the spins. These spins that have a random spatial distribution initially, couple to the molecular rotation J to produce a total angular momentum vector F, with a spatial alignment or orientation less than the

initial one[19]. Moreover, if the alignment or orientation of J can be repeatedly detected for different times form the optical excitation, a temporal beating is observed.

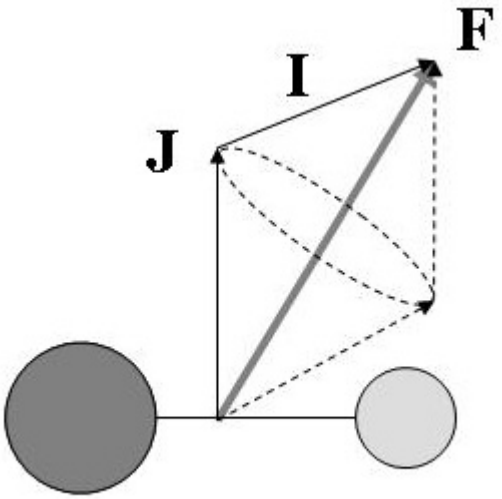

Figure 7: Coupling of the molecular rotational angular momentum J with the nuclear spin I to give F.

This behaviour obviously is a drawback in the use of pulsed laser excitation, especially when applied in the preparation of polarized reagents for the study of chemical reactivity, since the time that it takes for a macroscopic sample of gasses to react can be in the same order as these hyperfine beatings (typically in the order of μs due to the hyperfine coupling constants being in the order of hundreds of kHz). On the other hand, the fact that this behaviour is attributed to the nuclear spins, and the fact that angular momentum is a conservable magnitude give the unique opportunity to use this depolarization mechanism in order to polarize indirectly the nuclear spin.

Hyperfine beating cycles the nuclear polarization between zero and a maximum value, with the rotational polarization exhibiting the opposite behaviour. For some applications (such as gas-phase NMR of molecules), cycles of pumping, at a rate high enough to overcome the losses due to depolarizing collisions, can lead to the production of large steady-state nuclear polarizations in the parent molecules. Otherwise, photodissociating the molecule using a second laser pulse, carefully timed to coincide with a maximum in the nuclear polarization, allows the polarization at a given instant in time to be 'frozen in', producing highly polarized atomic nuclei. This

is in addition to the highly polarized *electronic* angular momentum that can arise from the photodissociation process itself [21,22,23]. Together, molecular state preparation followed by appropriately time-delayed photodissociation allows the production of highly polarized atoms at very high densities, close to the density of the parent molecules.

The quantitative description of this phenomenon can be maid with the use of the Wigner symbols, and in general with the algebra used for the description of quantum angular momentum. An introduction to this theory is not going to be given here, as it can be easily found in any angular momentum textbooks, with [24] being probably the most appropriate. Nevertheless, we describe in brief the formalism used, and also we present a very important theorem of quantum angular momentum, the Wigner-Eckart theorem, as well as two theorems that emerge from it and are very useful for the development of the equations that describe polarization transfer from rotation to the nuclear spin.

The description of the molecular rotation depolarization is going to be presented first, as it existed for many years before was this mechanism was proposed as a method for the polarization of the nuclear spin. The theoretical and experimental studies of depolarization of optically prepared molecules, provided with useful conclusions that form a qualitive view of the phenomena. Such a view is important in the search for molecular excitation schemes that can be used as sources of polarized atoms, since it helps to confine the search into the most promising systems. Finally, the equations that describe the nuclear spin polarization through this interaction are presented as an extension of the previously existed formalism and several examples of how this theory can be applied for the preparation of polarized atoms are given.

(B) DEPOLARIZATION OF OPTICALLY PREPARED REAGENTS

4. The $A_q^{(k)}(J)$ multipole moments, the Wigner-Eckart theorem and two useful theorems.

An angular momentum distribution may be described by the $(2J+1)^2$ density matrix elements $\rho_{m'm}$, or equivalently, by the $(2J+1)^2$ multipole moments $A_q^{(k)}(J)$, where k, which is limited to the integer values $0 \le k \le 2J$, is the order of the multipole moment. These two sets of parameters are related by the expressions

$$\rho_{m'm} = \sum_{k,q} \frac{(2k+1)[J(J+1)]^{k/2}}{c(k)\left\langle J \left\| J^{(k)} \right\| J \right\rangle} (-1)^{J+q-m'} \begin{pmatrix} J & k & J \\ -m & q & m' \end{pmatrix} A_q^{(k)}(J), \tag{1a}$$

and

$$A_q^{(k)}(J) = \frac{c(k)}{\left\langle Jm \left| \mathbf{J}^2 \right| Jm \right\rangle^{k/2}} \sum_{m,m'} \rho_{m'm} \left\langle Jm \left| J_q^{(k)} \right| Jm' \right\rangle, \tag{1b}$$

where the $\left\langle \mathrm{J} \left\| \mathrm{J}^{(\mathrm{k})} \right\| \mathrm{J} \right\rangle$ are the reduced matrix elements of the rotational angular momentum **J**, and the $J_q^{(k)}$ are the spherical tensor operators of the molecular rotation **J** [25].

The reduced matrix elements are defined through the widely known Wigner-Eckart theorem that can be stated as

$$\left\langle J,M \left| T(k,q) \right| J',M' \right\rangle = \left\langle kq,J',M' \left| J,M \right\rangle \left\langle J \left\| T_k \right\|, J' \right\rangle \right. \tag{2a}$$

or equivalently as

$$\left\langle J,M \left| T(k,q) \right| J',M' \right\rangle = (-1)^{j'-m'} \begin{pmatrix} j' & k & j \\ -m' & q & m \end{pmatrix} \left\langle J \left\| T_k \right\| J' \right\rangle \tag{2b}$$

The Wigner-Eckart theorem states that the physical problem represented by the matrix element of a tensor operator in some basis, can be separated into two components, one associated with the geometry, embodied in the Clebsch-Gordon

coefficient, and one with the dynamics of the system embodied in the reduced matrix element [19].

The Wigner-Eckart theorem can be very useful in the case of composite tensor operators acting in coupled angular momentum spaces. For example let us consider a composite tensor operator $X^{k}_{q} = \left[T^{k_1} \otimes T^{k_2}\right]^{k}_{q} = \sum_{q_1,q_2} \langle k_1\, q_1, k_2\, q_2 | k\, q, \rangle T^{k_1}_{q_1}\, T^{k_2}_{q_2}$ that consist of the tensor operators $T^{k_1}\ \ T^{k_2}$ each of them acting in $|j_1 m_1\rangle$ and $|j_2 m_2\rangle$ states. The coupled basis in which the composite tensor operator acts can be constructed as $|j_1, j_2, j, m\rangle = \sum_{m_1,m_2} \langle j_1\, m_1, j_2\, m_2 \,|\, j\, m\rangle |j_1\, m_1\rangle |j_2\, m_2\rangle$. Using the W.E theorem we can write for the reduced matrix element of the composite operator

$$\langle j_1\, j_2\, j \| X^{k} \| j_1'\, j_2'\, j' \rangle = \sqrt{(2j+1)(2j'+1)(2k+1)} \begin{Bmatrix} j_1 & j_1' & k_1 \\ j_2 & j_2' & k_2 \\ j & j' & k \end{Bmatrix} \langle j_1 \| T^{k_1} \| j_1' \rangle \langle j_2 \| T^{k_2} \| j_2' \rangle \tag{3}$$

This is a special case of the formula 14.66 derived in [26] and we will refer to it as SM(14.66).

There are also cases where a composite tensor operator $X^{k}_{q} = \left[T^{k_1} \otimes T^{k_2}\right]^{k}_{q}$ is comprised out of two (or more) tensor operators, all acting in the same basis $|j\, m\rangle$. The reduced matrix element of such a tensor can be written as

$$\left\langle j \left\| \left[T^{k_1} \otimes T^{k_2}\right]^{k} \right\| j' \right\rangle = (-1)^{j+j'+k} \sqrt{2k+1} \sum_{j''} \left\langle j \left\| T^{k_1} \right\| j'' \right\rangle \left\langle j'' \left\| T^{k_2} \right\| j' \right\rangle \begin{Bmatrix} j & j' & k \\ k_2 & k_1 & j'' \end{Bmatrix} \tag{4}$$

This is a special case of the theorem given in [27] in equation 15.15 and will be referred to as FR(15.15).

An advantage in using the $A^{(k)}_{q}(J)$ multipole moments to describe angular momentum distributions comes from the fact that they can be easily combined with the tensor operator representation of an interaction, since they can depend on the same k,q parameters. For some circumstances the $A^{(k)}_{q}(J)$ multipole moments correspond to

directly measured observables. For example, multiple moments with a rank of zero correspond to the population in the particular J state of a distribution, odd ranks correspond to the distribution's orientation while even ranks to the distribution's alignment. Also, the average value of the angular momentum projection distribution is directly proportional to the k=1 multipole moment. This can be seen if we write the average value of m in the density matrix representation

$\langle \mathrm{m} \rangle = \sum_{\mathrm{m}=-\mathrm{J}}^{\mathrm{J}} \mathrm{m}\rho_{\mathrm{mm}}$ and we express the density matrix in terms of the $A_q^{(k)}(J)$ multipole moments according to equation 1a. We note that since m=m', q is constrained to be 0. Furthermore, the summation of the product of m, which is proportional to $\begin{pmatrix} J & 1 & J \\ -m & 0 & m \end{pmatrix}$, with the 3-j symbol $\begin{pmatrix} J & k & J \\ -m & 0 & m \end{pmatrix}$, over the range –J to J , is zero for all k except k=1 (due to the orthogonality of 3-j symbols, as expressed by equation. (2.32) in [20]. Using c(1)=1 [21], $\left\langle J \left\| J^{(1)} \right\| J \right\rangle = \sqrt{\mathrm{J(J+1)(2J+1)}}$, and $\begin{pmatrix} J & 1 & J \\ -m & 0 & m \end{pmatrix} = (-1)^{J-m} \frac{m}{\sqrt{J(J+1)(2J+1)}}$ [20], we find that:

$$\langle \mathrm{m} \rangle = \sum_{\mathrm{m}=-\mathrm{J}}^{\mathrm{J}} \frac{3\mathrm{m}^2}{(2\mathrm{J}+1)\sqrt{\mathrm{J(J+1)}}} \mathrm{A}_0^{(1)}(\mathrm{J})$$

The summation of m^2, over the range –J to J, yields J(J+1)(2J+1)/3, which then gives the final result, that the expectation value of m is proportional to the dipole moment of J:

$$\langle \mathrm{m} \rangle = \sqrt{\mathrm{J(J+1)}}\ \mathrm{A}_0^{(1)}(\mathrm{J}) \tag{5}$$

This way, the conservation of angular momentum projection of a molecular system comprised of N nuclei can be written as

$$\sqrt{J(J+1)}A_0^{(1)}(J) + \sqrt{I_1(I_1+1)}A_0^{(1)}(I_1) + \ldots + \sqrt{I_N(I_N+1)}A_0^{(1)}(I_N) = Const.$$

5. Calculation of the $G^k(J,t)$ depolarization coefficient.

The time dependence of the molecule's polarization is characterized by a time-dependent polarization factor, $G^{(k)}(J,t)$, that was originally derived in [19]. As described previously, a molecule for which the rotational angular momentum has been polarized following prompt preparation such as pulsed-laser excitation or as a product of a chemical reaction or photodissociation, is characterized by a time-dependent polarization factor, $G^{(k)}(J,t)$ defined as

$$G^{(k)}(J,t)=\frac{\left\langle J^{(k)}(t)\right\rangle}{\left\langle J^{(k)}(0)\right\rangle} \text{ or } G^{(k)}(J,t)=\frac{A_q^k(J,t)}{A_q^k(J,0)}. \tag{6}$$

We will examine the general case of diatomic, heteroatom molecules that contain atoms with nuclear spins I_1 and I_2. We can define the composite tensor operator $T^{(k)}(t)=I_2^{(0)}\cdot I_1^{(0)}\cdot J^{(k)}(t)$ that consists of the nuclear spin operators $I_{1,2}^{(0)}$ that act on the nuclear spin states $\left|I_{1,2}\, m_{1,2}\right\rangle$ and the rotational angular momentum tensor operator $J^{(k)}(t)$ that acts in the rotational angular momentum state $\left|J\, m_J\right\rangle$. The composite tensor operator $T^{(k)}(t)$ acts in the coupled basis $\left|F_i FM_F\right\rangle$ defined as

$$\left|I_2(I_1J)F_i,FM_F\right\rangle=\sum_{\substack{m_1,m_2,m_3,\\ M_{F_i}}}\left\langle I_1\, m_1, J\, m_J\left|F_i\, M_{F_i}\right.\right\rangle\left\langle I_2\, m_2, F_i\, M_{F_i}\left|F\, M_F\right.\right\rangle\left|I_1\, m_1\right\rangle\left|I_2\, m_2\right\rangle\left|J\, m_J\right\rangle.$$

In the above definition we consider the following coupling order: first I_1 couples to J to produce the intermediate quantum number F_i which finally couples to I_2 to produce the total angular momentum quantum number F. The reason we choose this order is because it will suitable for the application of the hierarchical coupling approximation which is outlined as: For the general case of heteroatom molecules, one of the two nuclei, for example I_1, is more strongly coupled to the molecular rotation than the other. In the case where the coupling strength is very different, we can assume that the rotational depolarization is mainly caused by I_1 (hierarchical coupling limit). In this case, it is this nuclei the one that acquires most of the

molecule's polarization, while nuclei I_2 interacts with the averaged polarization of I_1 and J. Note that choosing this particular coupling order, we do not yet impose the hierarchical coupling or any other approximation, but simply, out of all the possible choices we choose the one that will allow us to study the hierarchical coupling limit more easily.

The time-dependence of the $G^{(k)}(J,t)$ factor can be obtained through the evaluation of the reduced matrix element $\left\langle I_2(I_1J)F_iF\left\|T^{(k)}(t)\right\|I_2(I_1J)F_i'F'\right\rangle$. We can evaluate $\left\langle I_2(I_1J)F_iF\left\|T^{(k)}(t)\right\|I_2(I_1J)F_i'F'\right\rangle$ with applying twice equation S(14.66) and then invert, to take the reduced matrix element of interest

$$\left\langle J\left\|J^{(k)}(t)\right\|J\right\rangle\left\langle I_1\left\|I_1^{(0)}\right\|I_1\right\rangle\left\langle I_2\left\|I_2^{(0)}\right\|I_2\right\rangle=\sum_{\substack{F_i,F_i'\\F,F'}}\left\langle I_2(I_1J)F_iF\left\|T^{(k)}(t)\right\|I_2(I_1J)F_i'F'\right\rangle$$
$$\times((I_2I_2)0(F_iF_i')k\,|\,(I_2F_i)F(I_2F_i')F')^{(k)}$$
$$\times((I_1I_1)0(JJ)k\,|\,(I_1J)F_i(I_1J)F_i')^{(k)}$$

where the reducing 9j symbols produced with the application of S(14,66) have been collected to the more compact symbols

$$((II)0(JJ)k\,|\,(IJ)F(IJ')F')^{(k)}=\sqrt{\frac{(2F+1)(2F'+1)}{2I+1}}(-1)^{I+J'+F+k}\begin{Bmatrix}J' & F' & I\\ F & J & k\end{Bmatrix}.$$

The operator $T_q^{(k)}$ can also be expressed in the Heisenberg picture as $T^{(k)}(t)=\exp(iHt/\hbar)T^{(k)}(0)\exp(-iHt/\hbar)$ so that the time dependent matrix element can be evaluated after application of FR(15.15)

$$\left\langle I_2(I_1J)F_iF\left\|\exp(iHt/\hbar)T^{(k)}(0)\exp(-iHt/\hbar)\right\|I_2(I_1J)F_i'F'\right\rangle=$$
$$\sum_{F_i'',F_i'''}\frac{\left\langle I_2(I_1J)F_iF\left\|\exp(iHt/\hbar)\right\|I_2(I_1J)F_i''F\right\rangle}{\sqrt{2F+1}}$$
$$\times\left\langle I_2(I_1J)F_i''F\left\|T^{(k)}(0)\right\|I_2(I_1J)F_i'''F'\right\rangle$$
$$\times\frac{\left\langle I_2(I_1J)F_i'''F'\left\|\exp(-iHt/\hbar)\right\|I_2(I_1J)F_i'F'\right\rangle}{\sqrt{2F'+1}}$$

where the evolution operators $e^{\pm\frac{iHt}{t}}$ have been treated as tensor operators of zero order, a fact that explains the absence of 6j symbols form the formula above. The reduced matrix elements of $e^{\pm\frac{iHt}{t}}$ are evaluated by finding the representation for which the Hamiltonian is diagonal. They become ordinary matrix elements according

to $\dfrac{\left\langle F_i F \left\| e^{\frac{iHt}{t}} \right\| F_i' F \right\rangle}{\sqrt{2F+1}} = \left\langle F_i F\, M_F \left| e^{\frac{iHt}{t}} \right| F_i' F\, M_F \right\rangle$ which can be evaluated for any value of M_F. In terms of the eigenvalues and the eigenvectors $C^{(F)}_{F_i,\alpha} = \left\langle I_2 (I_1 J) F_i, FM_F \,|\, (I_2 I_1 J)\alpha, FM_F \right\rangle$ obtained by the diagonalization of H we can write $\dfrac{\left\langle F_i F \left\| e^{\frac{iHt}{t}} \right\| F_i' F \right\rangle}{\sqrt{2F+1}} = \sum_\alpha C^{(F)}_{F_i,\alpha} e^{i\frac{Et}{\hbar}} C^{(F)*}_{F_i',\alpha'}$.

The time-independent term $\left\langle I_2 (I_1 J) F_i'' F \left\| T^{(k)}(0) \right\| I_2 (I_1 J) F_i''' F' \right\rangle$ again with applying equation S(14.66)

$$\left\langle I_2 (I_1 J) F_i'' F \left\| T^{(k)}(0) \right\| I_2 (I_1 J) F_i''' F' \right\rangle = \left\langle J \left\| J^{(k)}(0) \right\| J \right\rangle \left\langle I_1 \left\| I_1^{(0)} \right\| I_1 \right\rangle \left\langle I_2 \left\| I_2^{(0)} \right\| I_2 \right\rangle$$
$$\times ((I_2 I_2) 0 (F_i'' F_i''') k \,|\, (I_2 F_i'') F (I_2 F_i''') F')^{(k)}$$
$$\times ((I_1 I_1) 0 (JJ) k \,|\, (I_1 J) F_i'' (I_1 J) F_i''')^{(k)}$$

Putting all terms together we take the expression for $G^{(k)}(J,t)$

$$\mathrm{G^{(k)}(J,t)} = \sum_{\substack{\mathrm{F,F'} \\ \alpha,\alpha'}} \frac{(2\mathrm{F}+1)(2\mathrm{F'}+1)}{(2\mathrm{I}_1+1)(2\mathrm{I}_2+1)} \cos\left[\frac{\left(\mathrm{E}_{\alpha,\mathrm{F}} - \mathrm{E}_{\alpha',\mathrm{F'}}\right)\mathrm{t}}{\hbar}\right]$$
$$\left(\sum_{\mathrm{Fi,Fi'}} (-1)^{\mathrm{F_i+F_i'}} \sqrt{(2\mathrm{F_i}+1)(2\mathrm{F_i'}+1)} \begin{Bmatrix} \mathrm{F_i'} & \mathrm{J} & \mathrm{I_1} \\ \mathrm{J} & \mathrm{F_i} & \mathrm{k} \end{Bmatrix} \begin{Bmatrix} \mathrm{F_i'} & \mathrm{F'} & \mathrm{I_2} \\ \mathrm{F} & \mathrm{F_i} & \mathrm{k} \end{Bmatrix} \mathrm{C^{(F)}_{F_i,\alpha} C^{(F')*}_{F_i',\alpha'}} \right)^2 \qquad (7)$$

For many applications it is useful to calculate the average depolarization due to the nuclear spins. This is obtained by removing from equation 6 all the terms for which $E_{F_i,\alpha} \neq E_{F_i',\alpha'}$ and results to

$$G^{(k)} = [(2I_1+1)(2I_2+1)]^{-1} \sum_{\alpha,F} (2F+1)^2$$
$$\times \left| \sum_{F_i,F_i'} (-1)^{F_i+F_i'} \sqrt{(2F_i+1)(2F_i'+1)} C^{(F)}_{F_i,\alpha} C^{(F)*}_{F_i',\alpha'} \begin{Bmatrix} F_i' & J & I_1 \\ J & F_i & k \end{Bmatrix} \begin{Bmatrix} F_i' & F & I_2 \\ F & F_i & k \end{Bmatrix} \right|^2 \qquad (8)$$

The Hierarchical approximation that we mentioned before can be imposed if we consider the coupled representation $\left|I_2(I_1J)F_i, FM_F\right\rangle$ to be the basis for which the Hamiltonian is diagonal. In this case we replace $C^{(F)}_{F_i,\alpha} \to \delta_{\alpha,F_i}$ and we obtain the hierarchical approximation formula for $G^{(k)}(J,t)$ to be

$$G^{(k)}(J,t) = \sum_{F,F'} \sum_{F_i,F_i'} \frac{(2F+1)(2F'+1)(2F_i+1)(2F_i'+1)}{(2I_1+1)(2I_2+1)} \begin{Bmatrix} F_i' & J & I_1 \\ J & F_i & k \end{Bmatrix}^2 \begin{Bmatrix} F_i' & F' & I_2 \\ F & F_i & k \end{Bmatrix}^2 \cos\left[\frac{\left(E_{F_i,F} - E_{F_i',F'}\right)t}{\hbar}\right] \tag{9}$$

In the simplest case where the molecule possesses one or more indistinguishable nuclei, or only one of the nuclei has non zero spin (i.e. $I_2 = 0$ and I_1=I), Equation (7) is simplified and the molecular depolarization is described by:

$$G^{(k)}(J,t) = \sum_{F,F'} \frac{(2F+1)(2F'+1)}{(2I+1)} \begin{Bmatrix} F' & F & k \\ J & J & I \end{Bmatrix}^2 \cos\left[\frac{\left(E_F - E_{F'}\right)t}{\hbar}\right] \tag{10}$$

6. Application to molecular depolarization

As discussed in the introduction, the use of optically aligned reagents in studies of chemical reactivity consisted one of the main initiatives for the observation and the detailed study of hyperfine depolarization in molecular systems. It has been explained qualitatively that the degree of anisotropy achieved via optical excitation will be limited by the randomly oriented nuclear spins. The quantitative analysis of depolarization in several systems, allows us to extract some more general conclusions that are important in the design of experiments that make use of optically prepared reagents and can guide us to choose the most appropriate systems, in which we can exploit this depolarization effect to prepare atomic gasses with polarized nuclear spin.

a) Systems with one indistinguishable nuclear spin.

The less complicated situation where depolarization due to the hyperfine coupling can be observed is when the system contains one nuclei or one indistinguishable nuclear spin. Such a situation is described by equation 10 and perhaps the it's most simple application is the description of the electron spin depolarization due to the nuclear spin as this occurs when the electron spin is polarized via photodissociation with circularly polarized light. In such an example the electron spin is depolarized thus it takes the role of rotational angular momentum. Since the only two angular momentum entities equal to ½ there is only one non-zero term and the resulting beating is a very simple cosine with a frequency of as expected (the frequency corresponds to the same transition that generates the 21cm background radiation).

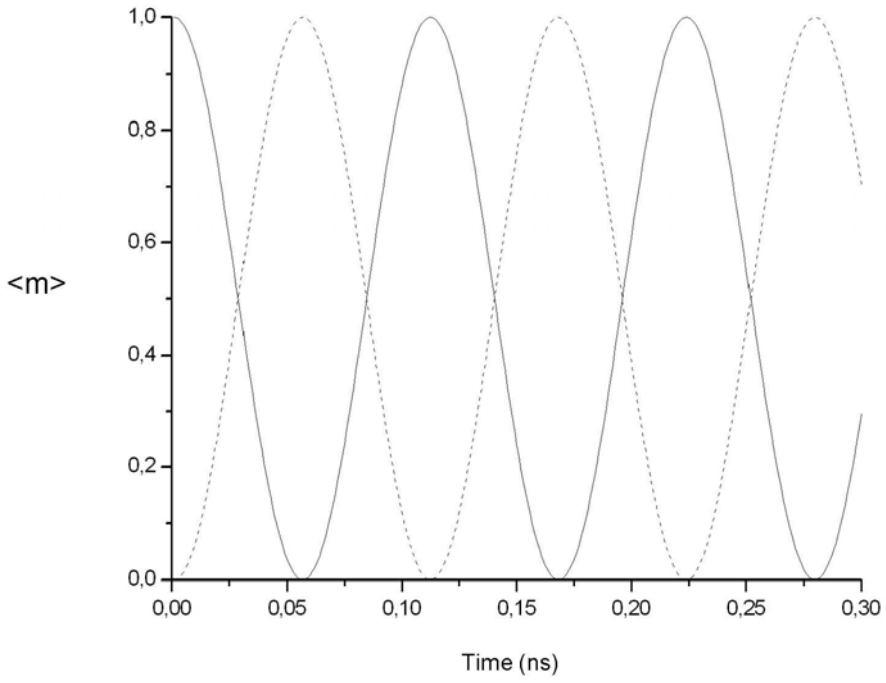

Figure 8: Depolarization of the electron spin to the nuclear spin due to the hyperfine interaction.

The same formula describes the molecular rotation depolarization in a system with two indistinguishable nuclei as H_2. Of course now the hyperfine structure is more complicated since there are two angular momentum entities involved J that corresponds to the molecular rotation and I_R that corresponds to the total nuclear spin, and they both equal to one. This treatment assumes that J interacting with the total nuclear spin which is 1 (orthonormal case) while the molecules where I_R equals 0 (paranormal case) exhibits no hyperfine structure and consequently no depolarization. The hyperfine structure for H_2 is

$$\frac{H}{h} = -c\left(I_R\ J\right) + d\left\{3\left(I_R\ J\right)^2 + \frac{3}{2}\left(I_R\ J\right) - I_R^2\ J^2\right\}$$

where $d = \dfrac{\mu_H^2\left\langle r^{-3}\right\rangle}{hI_1}\dfrac{\left(I_R\left(I_R+1\right)+4I_1\left(I_1+1\right)\right)}{\left(2I_R-1\right)\left(2I_R+3\right)\left(2J-1\right)\left(2J+2\right)}$ and I is the nuclear spin of one nuclei while I_R the total nuclear spin of the molecule. We note that the molecules with $I_R = 0$ (paranormal state) couple only to even rotational angular momentum J, while the molecules with $I_R = 1$ (orthonormal state) to the odd J. The value for c is c = 113.8 kHz while $\mu_H^2\left\langle r^{-3}\right\rangle$ = 72.1 kHz [28].

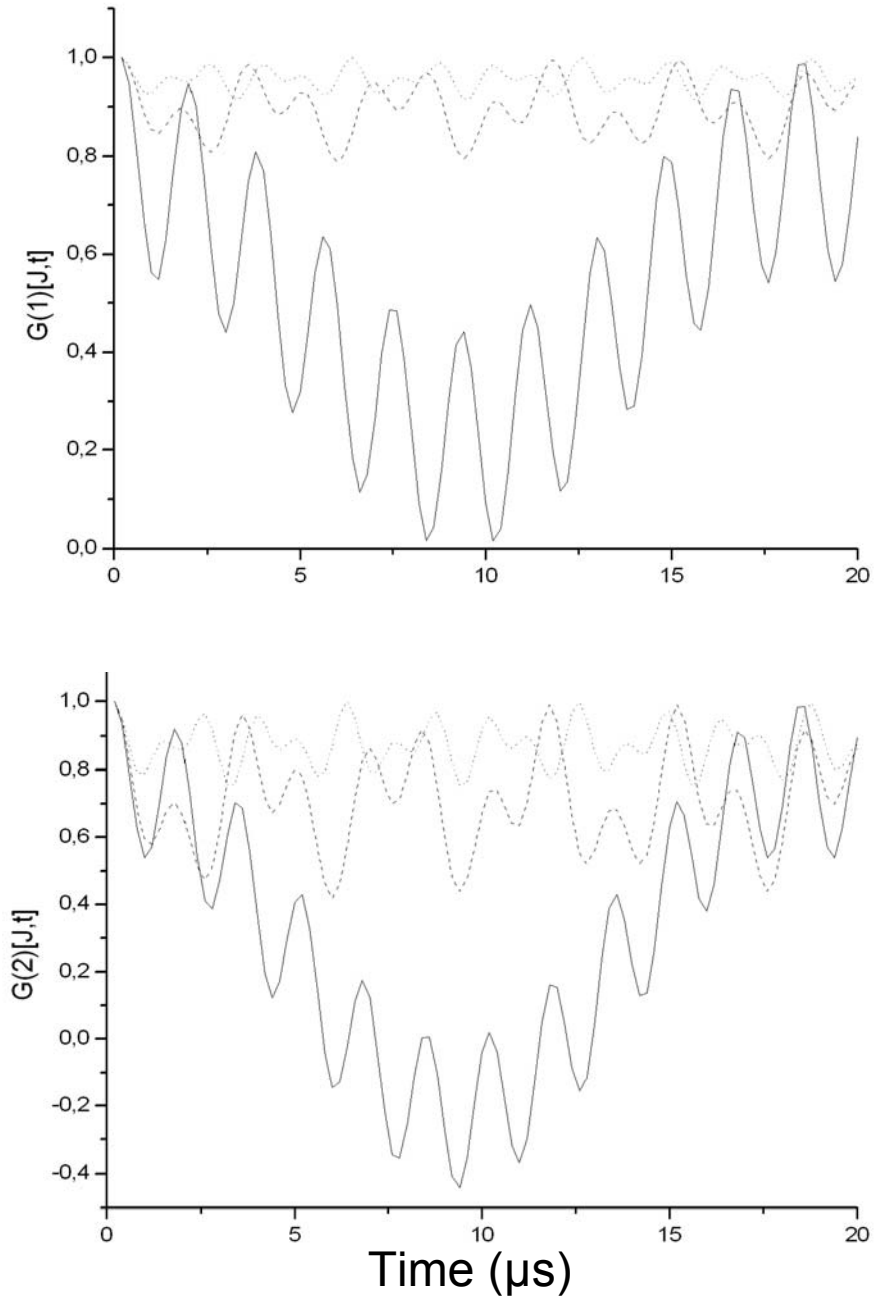

Figure 9: Depolarization of molecular rotation orientation and alignment for J = 1(bold line), 3(dashed line), 5(dotted line) for orthonormal H_2 molecule.

Another system that can also be described by equation 10 is acetylene C_2H_2. The hyperfine Hamiltonian is similar to the one of H_2 and the coupling constants are c = 3.58 kHz and $\mu_H^2\left\langle r^{-3}\right\rangle$ = 0.8 kHz [31]. Again, for $I_R = 0$ we have hyperfine coupling only to the J = 1 rotational states and for $I_R = 1$ to the even J states.

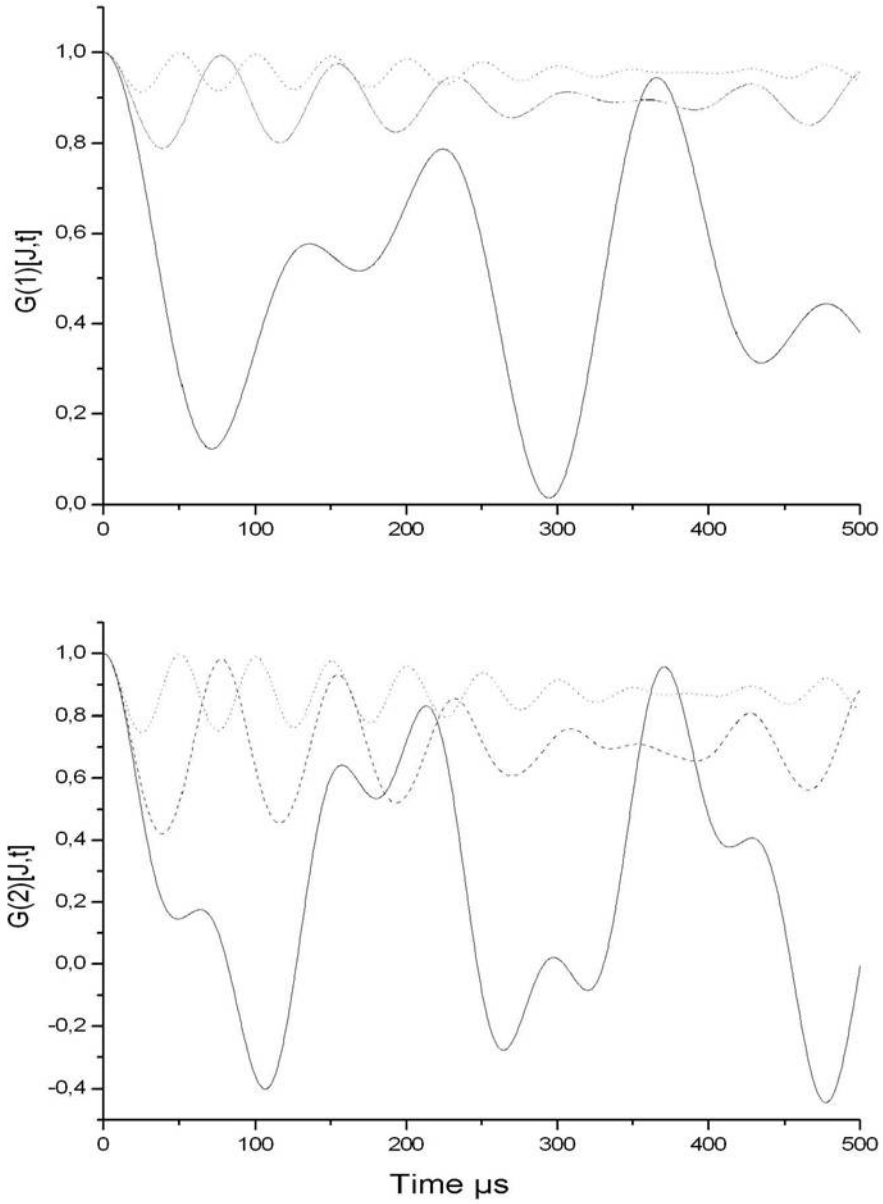

Figure 10: Depolarization of molecular rotation orientation and alignment for J = 1(bold line), 3(dashed line), 5(dotted line) for orthonormal C_2H_2 molecule.

Another system that contains one nuclear spin and thus is described by equation 10 is D_2. The difference between the hyperfine structure of D_2 and H_2 is that deuterium nuclei whose spin equals 1 exhibit quadrupolic coupling to the molecular rotation angular momentum. The hyperfine Hamiltonian will be

$$\frac{H}{h} = -c\left(I_R \ J\right) + d\left\{3\left(I_R \ J\right)^2 + \frac{3}{2}\left(I_R \ J\right) - I_R^2 \ J^2\right\}$$

Where d now equals to

$$d = \frac{1}{\left(2I_R - 1\right)\left(2I_R + 3\right)}$$
$$\times\left[\frac{\mu_H^2\left\langle r^{-3}\right\rangle}{hI_1}\frac{\left(I_R\left(I_R+1\right)+4I_1\left(I_1+1\right)\right)}{\left(2J-1\right)\left(2J+2\right)} + \frac{eqQ}{2hI_1(2I_1+1)}\left(1 - \frac{I_R(2I_R+1)+4I_1(2I_1+1)}{(2I_R-1)(2I_R+3)}\right)\right]$$

where c = 8.79 kHz, $\mu_H^2\left\langle r^{-3}\right\rangle$ = 6.8 kHz and eqQ = 224.9 kHz. The quadrupolic coupling constants are usually much larger than the magnetic dipole coupling constants. The depolarization of D_2 would be

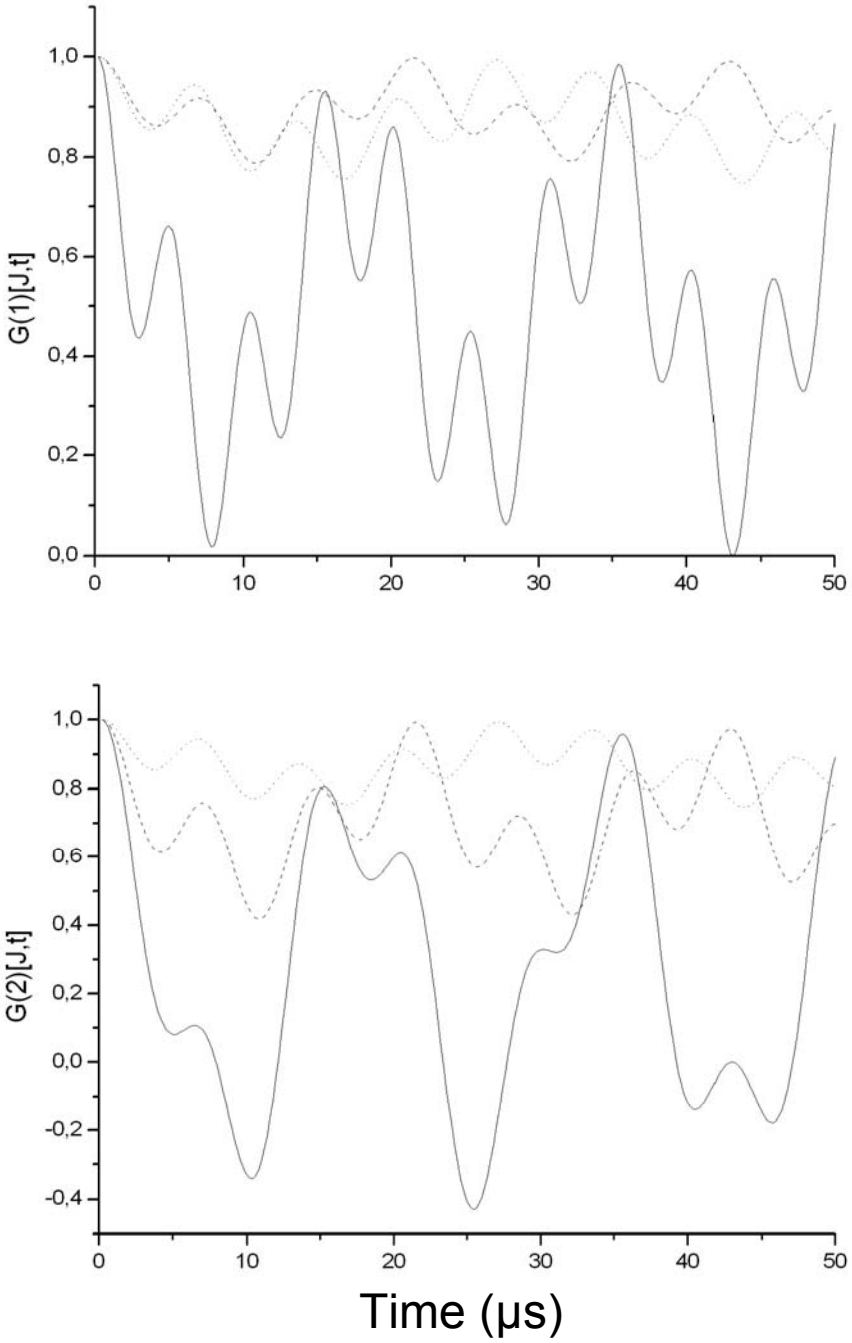

Figure 11: Depolarization of molecular rotation orientation and alignment for J = 1(bold line), 3(dashed line), 5(dotted line) for D_2.

c) Hydrogen-halides, deuterium-halides and the hierarchical approximation.

Molecular systems were two distinguishable nuclei are present, such as the hydro-halogen molecules are described by equations (7) or (9) depending on weather the hierarchical approximation can be applied or not. As an example we will consider the depolarization that follows the pulsed-infrared excitation of hydrogen fluoride. This is the same example considered in [16], while the hyperfine beating that results this situation have also been experimentally studied in [29].

Excitation of hydrogen fluoride through the transition HF(v=0,N')→HF(v=1,N) with linearly polarized light can produce various degrees of alignment that depended on the transitions chosen. For example, maximum degree of alignment can be achieved for N = 1 [16]. In generally, alignment can be described by the even order $A_q^{(k)}(J)$ multipole moments, and since k is limited to the integer values $0 \le k \le 2J$ we might as well describe the rotational alignment through $A_q^{(2)}(J)$. Since the temporal evolution of $A_q^{(k)}(J)$ is given by $A_q^{(k)}(J,t) = A_q^{(k)}(J,0)G^{(k)}(J,t)$ we can account for the hyperfine depolarization of the rotational alignment through evaluation of $G^{(2)}(J,t)$.

For the evaluation of equation 6 the energies $E_{F_i,\alpha}$ and eigenvectors $C_{F_i,\alpha}^{(F)}$ have to be calculated. Their values depend on the structure of the hyperfine Hamiltonian which in the absence of electromagnetic fields is

$$H = C_F I_F \cdot J \; + \; C_H I_H \cdot J \; + \; J_{HF} I_H \cdot I_F \; +$$
$$[S_{HF}/(2J+3)\,(2J-1)][\,3\,(I_H \cdot J)\,(I_F \cdot J) \; + \; 3\,(I_F \cdot J)\,(I_H \cdot J) \; - \; 2\,(I_H \cdot I_F)\,J\,(J+1)]$$

As we see, each nuclear spin couples to the magnetic field induced by the molecular rotation and also to each other, while there is also a more complex term that describes the coupling of one nuclear magnetic moment in the magnetic field of the other spin-spin interaction [31].

The values for the various constants, (that we will call hyperfine constants) have been extracted experimentally with frequency stabilized colour centered laser studies in HF by *Breant et al* [39]. This study reveals that the hyperfine constants are significantly varied between different vibrational states, a fact that explains why in we kept track of the vibration quantum number above. For the lowest vibrational state *v* =

0, and the first excited rotational state *J = 1* the values for the hyperfine structure constants are C_F *= 307.637 kHz,* C_H *= -71.128 kHz,* S_{HF} *= 28.675 kHz* , and J_{HF} = 0.529 *kHz* while the corresponding values for higher vibrational and rotational states are calculated as:

$$C_{H,F}(v,J) = C_{H,F}(v=0, J=0) + a_{H,F} \cdot v + b_{H,F} J(J+1)$$

with $a_F = 53\ kHz, \quad a_H = 1.99\ kHz, \quad b_F = 0.17\ kHz, \quad b_H = 0.036\ kHz$.

In the following figure we plot the $G^{(2)}(J,t)$ coefficient for several values of J.

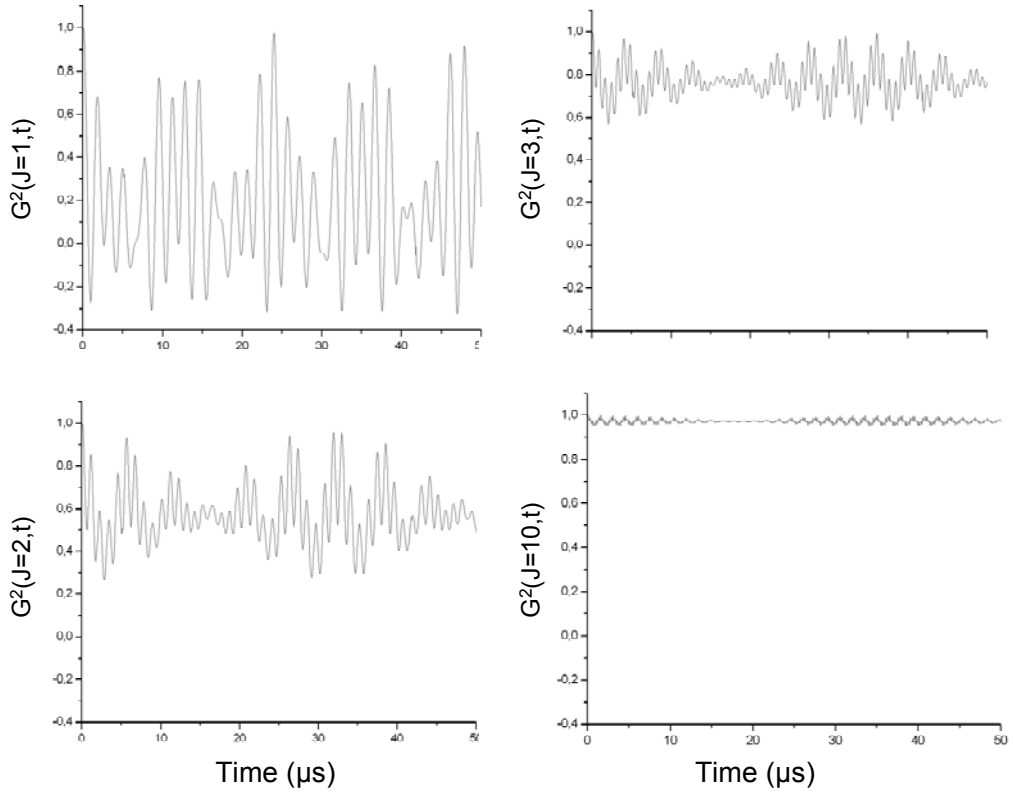

Fig12: Evolution of the depolarization coefficient G for rotational excitation J 1, 2, 3 and 10. The coefficient describes the time evolution of the alignment under the influence of the hyperfine interaction between the rotation and the nuclear spins.

In all the previous examples we notice one common characteristic. We see that for excitation to the lower rotational states the effect of hyperfine depolarization is strong while it is much less important for excitation to the higher states. This is a general characteristic for the hyperfine depolarization process and it can be qualitatively explained a "classical" argument: for excitation in the lower rotation states the rotational angular momentum vector size is comparable to the size of the vectors characterizing the nuclear spins, so the total angular momentum vector F and the rotation angular momentum number differ significantly. On the other hand, for higher rotation excitation, $J \approx F$ and the effect is much less important.

This hyperfine depolarization effect produces a beating in a microsecond timescale, as expected by the values of the hyperfine constants which are in the order of some hundreds of kHz. The timescale that characterizes depolarization in this system is such that would not affect measurements that occur in nanosecond timescale which is the usual pulse duration for the commonly used for spectroscopy lasers. On the other hand, if the aligned molecules are to be used as reagents in reactions with duration in the order of microseconds, the depolarization effects are expected to be important and have to be considered. Usually this is done by calculating the average depolarization due to the nuclear spins. Using equation (8) we obtain the following averaged depolarization and average alignment coefficients for hydrogen fluoride.

J	**$A^{(2)}_0(0)$**	**(Averaged)$G^{(2)}$**	**(Averaged) $A^{(2)}_0$**
1	-1	0.195	-0.195
2	-0.7	0.574	-0.402
3	-0.6	0.768	-0.461
4	-0.55	0.857	-0.471
5	-0.52	0.903	-0.470
10	-0.46	0.973	-0.488

In order to obtain the results presented in this paragraph we have used equation (7), which provides the general, non approximating solution. On the other hand, we notice that the hyperfine constant C_F which characterizes the fluorine's nuclear spin coupling to the molecular rotation is more than five times larger than C_H that characterizes the proton spin coupling to rotation. It would be therefore useful to

compare the solution provided by equation (7) with the hierarchical approximation solution provided by equation (9).

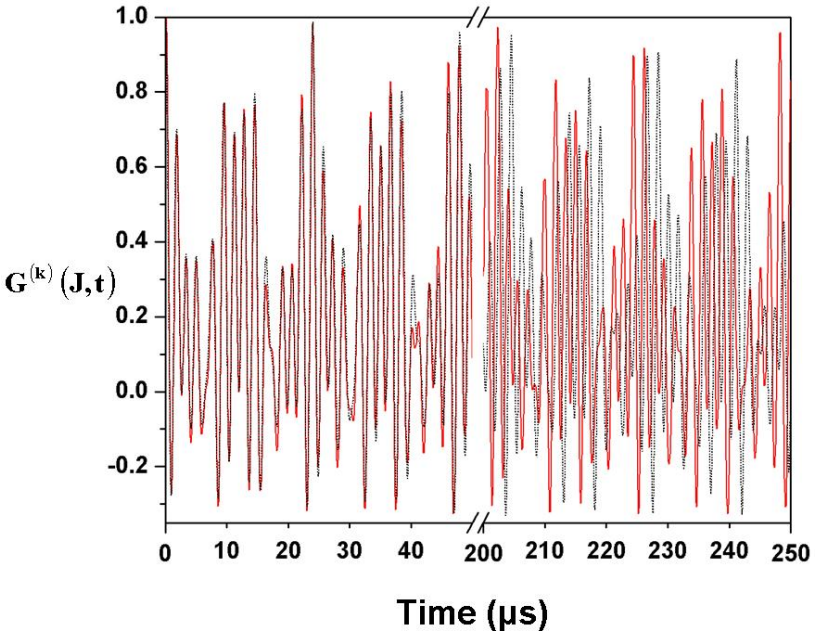

Figure 13: The molecular depolarization factor $G^{(2)}(J,t)$ that determines the time-dependence of the rotational alignment of HF, as calculated from the general non-hierarchical expression of Eq. 7 (solid red line), and from the hierarchical approximation of Eq. 9 (dashed black line).

We see the time dependence of the $G^{(2)}(J,t)$ factors, which describe the depolarization of the alignment of the HF (v = 1, J = 1 ,m=1) state. As we see, significant disagreement between the hierarchical (Eq. 7) and non-hierarchical expression (Eq. 9) appear only in very large times, where the hierarchical approximation's solution appears somewhat slower. This is a natural consequence of the hierarchical approximation which implies that all the polarization exchange occurs through $\mathbf{F_i} = \mathbf{J} + \mathbf{I_1}$, which for HF is the dominant coupling, but not the only one. Of course, the differences shown here occur on time scales not interesting for most experimental purposes, nevertheless, it is useful to see how the two approaches perform in a real system.

The differences between the hierarchical approximation solution (equation 9) and the general non-hierarchical (equation 7) are more intense in the case of the pulsed excitation of the (v=0, J=1, m=1) state of DF. The hyperfine Hamiltonian for this system is almost the same as for HF, where we I_H, C_H, and S_{HF} by I_D, C_D, and S_{DF}. The big difference though, between those two molecular systems, is that the value of one for the nuclear spin of deuterium though allows quadrupolic interaction to take place. Thus we have to embody this interaction in our description, and we do so by adding the following term for the interaction of the quadrupole moment of I_D with J:

$$H_Q = -\left[\frac{(eqQ)_D}{2I_D(2I_D-1)(2J-1)(2J+3)}\right]\left[3(I_D\cdot J)^2+\frac{3}{2}(I_D\cdot J)-I_D{}^2J^2\right]$$

The hyperfine energies are calculated by using the constants C_F = 158.356 kHz, C_D = -5.755 kHz, S_{DF} = 4.434 kHz, J_{DF} = 0 (no experimental measurement is given), and $(eqQ)_D$ = 354.238 kHz [30], and I_D=1. We now expect that the validity of the hierarchical approximation solution will be limited since the quadrupole coupling constant of deuterium to rotation is only 2.3 times larges than the coupling constant of the fluorine nuclei.

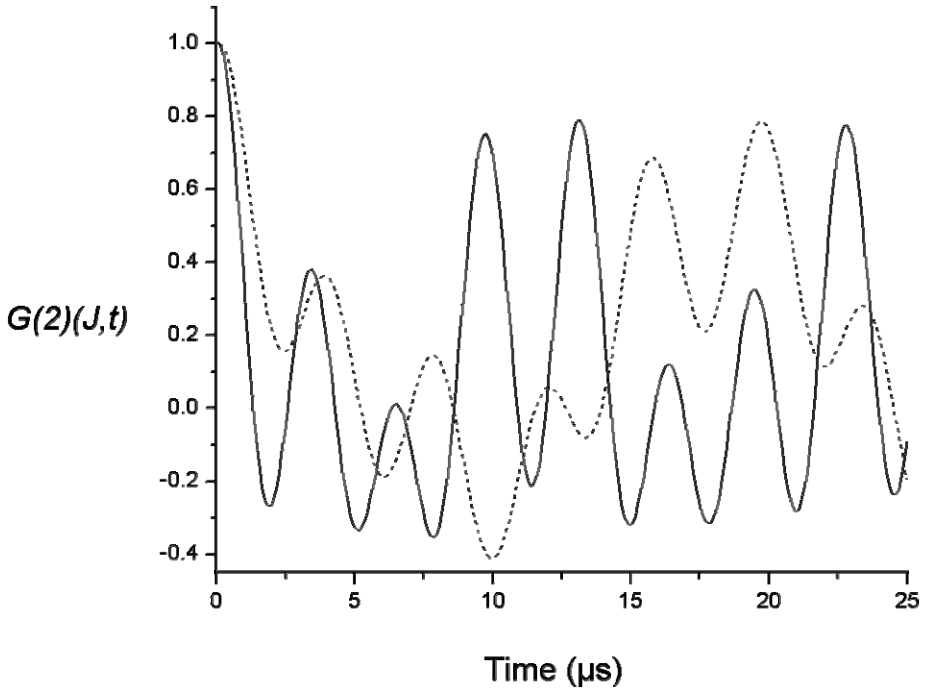

Figure 14: The molecular depolarization factor $G^{(2)}(J,t)$ that determines the time-dependence of the rotational alignment of DF, as calculated from the general non-hierarchical expression of Eq. 7 (solid line), and from the hierarchical approximation of Eq. 9 (dashed line).

As we see in the figure above, the approximate is now significantly slower than the exact solution, even in early times. Note that the quadruple interaction has been taken into consideration in both cases, the differences occur form the "weighting" of the several cosine functions involved, which is generated by the eigenvectors $C_{F_i,\alpha}^{(F)}$, which are absent in the approximate solution.

It would be difficult to extract a general rule for the use of one solution or the other. The reason that the example of DF has been chosen is to illustrate that the presence of quadruple interaction, which is usually much larger than the dipole interaction, is not a sufficient reason to adopt the approximating solution. That is because in this case the quadruple interaction of the deuterium nuclei acts to "balance" the coupling between the fluorine nuclei and the molecular rotation, which is large due to the larger "overlap" between the electronic and nucleonic wavefunctions in this case.

Let us consider excitation of HCl and DCl to the first rotational state. The hyperfine Hamiltonian of HCl will be the same with the one of HF except that now we have to take into consideration the quadrupole coupling exhibited by the chlorine nuclei which has spin 3/2. Thus we have to add the term

$$H_Q = -\left[\frac{(eqQ)_{Cl}}{2I_{Cl}(2I_{Cl}-1)(2J-1)(2J+3)}\right]\left[3(I_{Cl}J)^2+\frac{3}{2}(I_{Cl}J)-I_{Cl}{}^2J^2\right]$$

where the hyperfine constants are C_{Cl} = 58.6 kHz, C_H = 41 kHz, S_{HCl} = 1.081 kHz and eqQ_{Cl} = 69272 kHz [31]. Similarly the hyperfine structure of DCl will be the same with the one of HCl plus the term describing the quadrupole coupling exhibited by the deuterium nuclei whose spin is 1. Thus we add

$$\mathrm{H_Q} = -\left[\frac{\left(\mathrm{eqQ}\right)_{\mathrm{D}}}{2\mathrm{I_D}\left(2\mathrm{I_D}-1\right)\left(2\mathrm{J}-1\right)\left(2\mathrm{J}+3\right)}\right]\left[3\left(\mathrm{I_D}\cdot\mathrm{J}\right)^2+\frac{3}{2}\left(\mathrm{I_D}\cdot\mathrm{J}\right)-\mathrm{I_D}^2\mathrm{J}^2\right]$$

And the corresponding hyperfine constants for this system are C_{Cl} = 27.24 kHz, C_D = 3.29 kHz, S_{DCl} = 0.129 kHz, eqQ_{Cl} = 67393 kHz and eqQ_D = 187.36 kHz also taken by [31]. We can see that for these systems the hierarchical approximation is reasonable, since the constants characterizing the chorine's nucleus coupling to the rotation are much larger than the ones characterizing the proton's coupling. In the case of HCl the quadrupolic coupling "favors" chlorine's nucleus while the presence of quadrupolic coupling of deuterium nucleus in the case of DCl does not suffice to "balance" the system in a way that the hierarchical approximation is no longer valid.

Actually, the presence of quadrupolic coupling of deuterium nucleus hardy alters the depolarization time dependence.

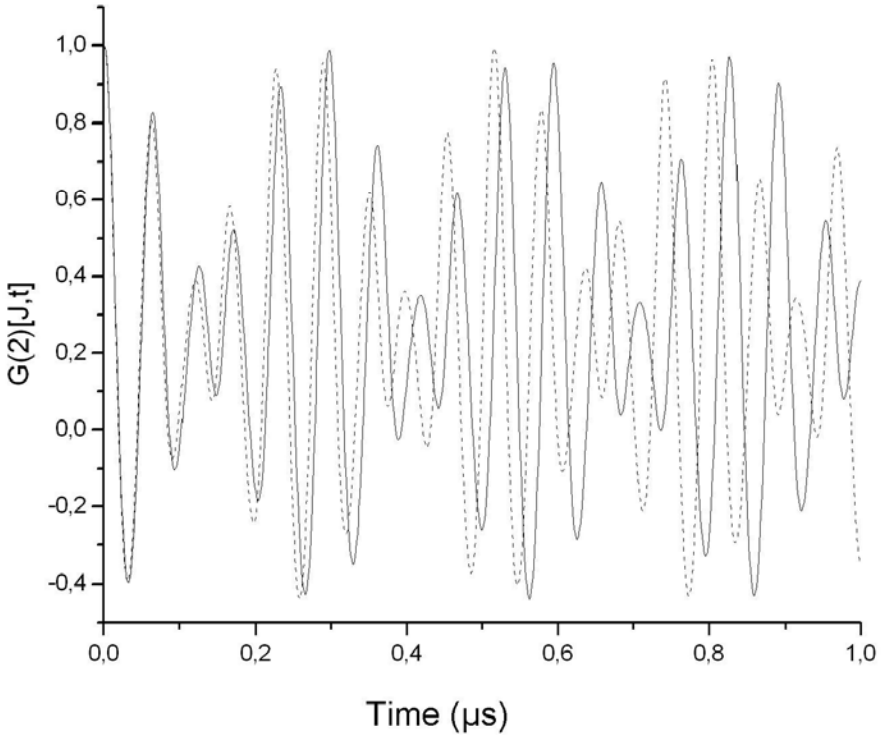

Figure 15: The molecular depolarization factor $G^{(2)}(J,t)$ for HCl (solid line), and for DCl (dashed line).

The approximate hierarchical formulas apply in the case where the coupling of one nuclear spin is much stronger than the others. All of the hydrogen halides except HF exhibit strong quadrupole coupling for the halogen nuclei so that the polarization dependence is very well described by the hierarchical expression. Even in the case of HF, where $I_F=1/2$ and does not possess a quadrupole moment, we find that the hierarchical approximation is still quite accurate. On the other hand, the general, non approximating formalism will be necessary for molecules for which the coupling strengths of the two nuclei is closer than DF, for example for molecules consisting of two isotopes of the same nuclei such as $^{35}Cl^{37}Cl$, HD, HT etc. The simplest possible situation is when the molecule possesses one non-zero nuclear spin, or possesses two or more indistinguishable nuclei. In such cases, for example OH, H_2 or CH_4, formula (10) applies.

(C) Polarizing the nuclear spin through the hyperfine interaction.

3. Calculation of the $H^{(k)}_{[1,2]}(I_{1,2},t)$ polarization coefficients (time-dependence of nuclear-spin polarization).

We need to calculate the time-dependent factors $H^{(k)}_{[1,2]}(I_{1,2},t)$ that characterize the nuclear spin polarization due to the polarization transfer from molecular rotation. These factors are similar to the $G^{(k)}(J,t)$ depolarization factor and are similarly calculated. To do so though, we need to develop a more straightforward approach than the one developed in [19] since the $H^{(k)}_{[1,2]}(I_{1,2},t)$ factors are in general more complicated. The new approach lies in the observation that

$$G^{(k)}(J,t)=\frac{\left\langle J^{(k)}(t)\right\rangle}{\left\langle J^{(k)}(0)\right\rangle}=\frac{\left\langle F_i\ F\left\|T^{(k)}(t)\right\|F_i'\ F'\right\rangle}{\left\langle F_i\ F\left\|T^{(k)}(0)\right\|F_i'\ F'\right\rangle} \tag{11}$$

which can be shown as

$$\frac{\left\langle F_i\ F\left\|T^{(k)}(t)\right\|F_i'\ F'\right\rangle}{\left\langle F_i\ F\left\|T^{(k)}(0)\right\|F_i'\ F'\right\rangle}=$$

$$\frac{\sqrt{(2k+1)(2F+1)(2F'+1)}\left\langle I_2\left\|I_2^{(0)}\right\|I_2\right\rangle\left\langle I_1\left\|I_1^{(0)}\right\|I_1\right\rangle\left\langle J\left\|J^{(k)}(t)\right\|J\right\rangle\begin{Bmatrix}I_1 & I_1 & 0\\ J & J & k\\ F_i & F_i' & k\end{Bmatrix}\begin{Bmatrix}I_2 & I_2 & 0\\ F_i & F_i' & k\\ F & F' & k\end{Bmatrix}}{\sqrt{(2k+1)(2F+1)(2F'+1)}\left\langle I_2\left\|I_2^{(0)}\right\|I_2\right\rangle\left\langle I_1\left\|I_1^{(0)}\right\|I_1\right\rangle\left\langle J\left\|J^{(k)}(0)\right\|J\right\rangle\begin{Bmatrix}I_1 & I_1 & 0\\ J & J & k\\ F_i & F_i' & k\end{Bmatrix}\begin{Bmatrix}I_2 & I_2 & 0\\ F_i & F_i' & k\\ F & F' & k\end{Bmatrix}}$$

$$=\frac{\left\langle J\left\|J^{(k)}(t)\right\|J\right\rangle}{\left\langle J\left\|J^{(k)}(0)\right\|J\right\rangle}=\frac{\sum_M\rho_M(-1)^{J-m}\begin{pmatrix}J & k & J\\ -M & q & M\end{pmatrix}\left\langle J\left\|J^{(k)}(t)\right\|J\right\rangle}{\sum_M\rho_M(-1)^{J-m}\begin{pmatrix}J & k & J\\ -M & q & M\end{pmatrix}\left\langle J\left\|J^{(k)}(0)\right\|J\right\rangle}=\frac{\left\langle J^{(k)}(t)\right\rangle}{\left\langle J^{(k)}(0)\right\rangle}.$$

The calculation of $G^{(k)}(J,t)$ is now simply evaluation of the reduced matrix element ratio (1).Using FR(15.15), the reduced matrix element in the numerator can be written as

$$\left\langle F_i F \left\| T^{(k)}(t) \right\| F_i' F' \right\rangle =$$

$$\left\langle F_i F \left\| e^{\frac{iHt}{t}} T^{(k)} e^{-\frac{iHt}{t}} \right\| F_i' F' \right\rangle = \sum_{F_i'', F_i'''} \frac{\left\langle F_i F \left\| e^{\frac{iHt}{t}} \right\| F_i'' F \right\rangle}{(2F+1)^{1/2}} \left\langle F_i'' F \left\| T^{(k)} \right\| F_i''' F' \right\rangle \frac{\left\langle F_i''' F' \left\| e^{-\frac{iHt}{t}} \right\| F_i' F' \right\rangle}{(2F'+1)^{1/2}}$$

The reduced matrix element $\left\langle F_i'' F \left\| T^{(k)} \right\| F_i''' F' \right\rangle$ can be expanded with the use of S(14.66)

$$\left\langle F_i'' F \left\| T^{(k)} \right\| F_i''' F' \right\rangle = \left\langle F_i'' F \left\| I_2^{(0)} \cdot I_1^{(0)} \cdot J^{(k)} \right\| F_i''' F' \right\rangle$$

$$= \sqrt{(2F+1)(2F'+1)(2F_i''+1)(2F_i'''+1)}(2k+1)$$

$$\left\langle I_2 \left\| I_2^{(0)} \right\| I_2 \right\rangle \left\langle I_1 \left\| I_1^{(0)} \right\| I_1 \right\rangle \left\langle J \left\| J^{(k)} \right\| J \right\rangle \begin{Bmatrix} I_1 & I_1 & 0 \\ J & J & k \\ F_i'' & F_i''' & k \end{Bmatrix} \begin{Bmatrix} I_2 & I_2 & 0 \\ F''_i & F_i''' & k \\ F & F' & k \end{Bmatrix}$$

while the denominator can be similarly written as

$$\left\langle F_i \; F \left\| I_2^{(0)} \cdot I_1^{(0)} \cdot J^{(k)} \right\| F_i' \; F' \right\rangle = \sqrt{(2F+1)(2F'+1)(2F_i'+1)(2F_i'+1)}(2k+1)$$

$$\left\langle I_2 \left\| I_2^{(0)} \right\| I_2 \right\rangle \left\langle I_1 \left\| I_1^{(0)} \right\| I_1 \right\rangle \left\langle J \left\| J^{(k)}(0) \right\| J \right\rangle \begin{Bmatrix} I_1 & I_1 & 0 \\ J & J & k \\ F_i & F_i' & k \end{Bmatrix} \begin{Bmatrix} I_2 & I_2 & 0 \\ F_i & F_i' & k \\ F & F' & k \end{Bmatrix}$$

Thus, the ratio in equation 5 takes the form

$$\frac{\left\langle F_i \; F \left\| I_2^{(0)} \cdot I_1^{(0)} \cdot J^{(k)}(t) \right\| F_i' \; F' \right\rangle}{\left\langle F_i \; F \left\| I_2^{(0)} \cdot I_1^{(0)} \cdot J^{(k)}(0) \right\| F_i' \; F' \right\rangle} =$$

$$\sum_{F_i'', F_i'''} \sqrt{(2F+1)(2F'+1)(2F_i''+1)(2F_i'''+1)}\,(2k+1)$$

$$\times \frac{\sum_{\alpha,\beta} C_{F_i\alpha}^{(F)} C_{F_i''\alpha'}^{(F)*} C_{F_i'''\beta}^{(F')} C_{F_i'\beta'}^{(F')*} \cos\left[\frac{E_{\alpha,F} - E_{\alpha',F'}}{\hbar} \cdot t\right] \begin{Bmatrix} I_1 & I_1 & 0 \\ J & J & k \\ F_i'' & F_i''' & k \end{Bmatrix} \begin{Bmatrix} I_2 & I_2 & 0 \\ F_i'' & F_i''' & k \\ F & F' & k \end{Bmatrix}}{\sqrt{(2F+1)(2F'+1)(2F_i'+1)(2F_i'+1)}(2k+1) \begin{Bmatrix} I_1 & I_1 & 0 \\ J & J & k \\ F_i & F_i' & k \end{Bmatrix} \begin{Bmatrix} I_2 & I_2 & 0 \\ F_i & F_i' & k \\ F & F' & k \end{Bmatrix}}$$

We multiply both the numerator and the denominator of this ratio with $\begin{Bmatrix} I_1 & I_1 & 0 \\ J & J & k \\ F_i & F_i' & k \end{Bmatrix} \begin{Bmatrix} I_2 & I_2 & 0 \\ F_i & F_i' & k \\ F & F' & k \end{Bmatrix} \sqrt{(2F+1)(2F'+1)(2F_i+1)(2F_i'+1)}(2k+1)$

and we sum over F_i, F, F_i', F' to obtain the orthonormality relation of the 9j symbols. After rearranging the terms and adopting the notation $F_i'' \to F_i$ $F_i''' \to F_i'$ we obtain for the depolarization coefficient

$$G^{(k)}(J,t) = \sum_{\substack{F,F' \\ \alpha,\alpha'}} \frac{(2F+1)(2F'+1)}{(2I_1+1)(2I_2+1)} \cos\left[\frac{\left(E_{\alpha,F} - E_{\alpha',F'}\right)t}{\hbar}\right]$$
$$\left(\sum_{Fi,Fi'} (-1)^{F_i+F_i'} \sqrt{(2F_i+1)(2F_i'+1)} \begin{Bmatrix} F_i' & J & I_1 \\ J & F_i & k \end{Bmatrix} \begin{Bmatrix} F_i' & F' & I_2 \\ F & F_i & k \end{Bmatrix} C^{(F)}_{F_i,\alpha} C^{(F')*}_{F_i',\alpha'}\right)^2$$

For many applications it is useful to calculate the average depolarization due to the nuclear spins. This is obtained by removing from equation 6 all the terms for which $E_{F_i,\alpha} \neq E_{F_i',\alpha'}$ and results to

$$G^{(k)} = [(2I_1+1)(2I_2+1)]^{-1} \sum_{\alpha,F} (2F+1)^2$$
$$\times \left| \sum_{F_i,F_i'} (-1)^{F_i+F_i'} \sqrt{(2F_i+1)(2F_i'+1)} C^{(F)}_{F_i,\alpha} C^{(F)*}_{F_i',\alpha'} \begin{Bmatrix} F_i' & J & I_1 \\ J & F_i & k \end{Bmatrix} \begin{Bmatrix} F_i' & F & I_2 \\ F & F_i & k \end{Bmatrix} \right|^2$$

The time dependence of the polarization of each nucleus is similarly governed by a time-dependent polarization factor, $H^{(k)}_{[i]}(I,t)$, which relates the spatial distribution of the nuclear spin, ***I***, with the original molecular polarization of ***J***: $A^{(k)}_q(I_j,t) = H^{(k)}_{[i]}(I,t)\, A^{(k)}_q(J,t=0)$. This polarization factor can be written as

$$H^{(k)}_{[1]}(I_1,t) = \frac{A^{(k)}_q(I_1,t)}{A^{(k)}_q(I_1,0)} =$$
$$\left(\frac{J(J+1)}{I_1(I_1+1)}\right)^{k/2} \frac{\langle I_1^{(k)}(t)\rangle}{\langle J^{(k)}(0)\rangle} = \left(\frac{J(J+1)}{I_1(I_1+1)}\right)^{k/2} \frac{\langle F_i\ F \| X^{(k)}(t) \| F_i'\ F'\rangle}{\langle F_i\ F \| T^{(k)}(0) \| F_i'\ F'\rangle} \qquad (12)$$

where $X^{(k)}(t)$ is a composite tensor operator of the form $X^{(k)}(t) = I_2^{(0)} I_1^{(k)}(t) J^{(0)}$, where the tensorial quantity k and the temporal evolution are embodied in the tensor

operator $I_1^{(k)}(t)$, whose average value temporal evolution we are trying to describe. In obtaining equation 9 we have used the definition of equation 7in [32]. Applying FR(15.15) we take for the time-dependent numerator

$$\left\langle F_i\ F\left\|I_2^{(0)}\cdot I_1^{(k)}(t)\cdot J^{(0)}\right\|F_i'\ F'\right\rangle =$$

$$\sum_{F_i'',F_i'''}\frac{\left\langle F_i\ F\left\|e^{\frac{iHt}{t}}\right\|F_i''\ F\right\rangle}{(2F+1)^{1/2}}\left\langle F_i''\ F\left\|I_2^{(0)}\cdot I_1^{(k)}(t)\cdot J^{(0)}\right\|F_i'''\ F'\right\rangle\frac{\left\langle F_i'''\ F'\left\|e^{-\frac{iHt}{t}}\right\|F_i'\ F'\right\rangle}{(2F'+1)^{1/2}}$$

while application of S(14.66) leads to

$$\left\langle F_i\ F\left\|I_2^{(0)}\cdot I_1^{(k)}(t)\cdot J^{(0)}\right\|F_i'\ F'\right\rangle=\left\langle I_2\left\|I_2^{(0)}\right\|I_2\right\rangle\left\langle I_1\left\|I_1^{(k)}\right\|I_1\right\rangle\left\langle J\left\|J^{(0)}\right\|J\right\rangle$$

$$\sum_{F_i'',F_i'''}\sqrt{(2F+1)(2F'+1)(2F_i''+1)(2F_i'''+1)}(2k+1)$$

$$\times\frac{\left\langle F_i\ F\left\|e^{\frac{iHt}{t}}\right\|F_i''\ F'\right\rangle}{(2F+1)^{1/2}}\begin{Bmatrix}I_1 & I_1 & k\\ J & J & 0\\ F_i'' & F_i''' & k\end{Bmatrix}\begin{Bmatrix}I_2 & I_2 & 0\\ F_i'' & F_i''' & k\\ F & F' & k\end{Bmatrix}\frac{\left\langle F_i'''\ F'\left\|e^{\frac{iHt}{t}}\right\|F_i'\ F'\right\rangle}{(2F'+1)^{1/2}}$$

The reduced matrix element $\left\langle F_i\ F\left\|T^{(k)}(0)\right\|F_i'\ F'\right\rangle$ can be evaluated application of S(14.66)

$$\left\langle F_i\ F\left\|I_2^{(0)}\cdot I_1^{(0)}\cdot J^{(k)}\right\|F_i'\ F'\right\rangle=\sqrt{(2F+1)(2F'+1)(2F_i'+1)(2F_i'+1)}(2k+1)$$

$$\left\langle I_2\left\|I_2^{(0)}\right\|I_2\right\rangle\left\langle I_1\left\|I_1^{(0)}\right\|I_1\right\rangle\left\langle J\left\|J^{(k)}(0)\right\|J\right\rangle\begin{Bmatrix}I_1 & I_1 & 0\\ J & J & k\\ F_i & F_i' & k\end{Bmatrix}\begin{Bmatrix}I_2 & I_2 & 0\\ F_i & F_i' & k\\ F & F' & k\end{Bmatrix}$$

Thus the ratio of the reduced matrix elements in [A.1] equals to

$$\frac{\left\langle F_i\ F\left\|I_2^{(0)}\cdot I_1^{(k)}(t)\cdot J^{(0)}\right\|F_i'\ F'\right\rangle}{\left\langle F_i\ F\left\|I_2^{(0)}\cdot I_1^{(0)}\cdot J^{(k)}(0)\right\|F_i'\ F'\right\rangle}=\frac{\left\langle I_1\left\|I_1^{(k)}\right\|I_1\right\rangle\left\langle J\left\|J^{(0)}\right\|J\right\rangle}{\left\langle J\left\|J^{(k)}(0)\right\|J\right\rangle\left\langle I_1\left\|I_1^{(0)}\right\|I_1\right\rangle}$$

$$\sum_{F_i'',F_i'''}\sqrt{(2F+1)(2F'+1)(2F_i''+1)(2F_i'''+1)}\,(2k+1)$$

$$\times\frac{\displaystyle\sum_{\alpha,\beta}C_{F_i\alpha}^{(F)}C_{F_i''\alpha'}^{(F)*}C_{F_i'''\beta}^{(F')}C_{F_i'\beta'}^{(F')*}\cos\left[\frac{E_{\alpha,F}-E_{\alpha',F'}}{\hbar}\cdot t\right]\begin{Bmatrix}I_1 & I_1 & k\\ J & J & 0\\ F_i'' & F_i''' & k\end{Bmatrix}\begin{Bmatrix}I_2 & I_2 & 0\\ F_i'' & F_i''' & k\\ F & F' & k\end{Bmatrix}}{\sqrt{(2F+1)(2F'+1)(2F_i'+1)(2F_i''+1)}(2k+1)\begin{Bmatrix}I_1 & I_1 & 0\\ J & J & k\\ F_i & F_i' & k\end{Bmatrix}\begin{Bmatrix}I_2 & I_2 & 0\\ F_i & F_i' & k\\ F & F' & k\end{Bmatrix}}$$

We multiply both the numerator and the denominator of this ratio with:

$$\begin{Bmatrix}I_1 & I_1 & 0\\ J & J & k\\ F_i & F_i' & k\end{Bmatrix}\begin{Bmatrix}I_2 & I_2 & 0\\ F_i & F_i' & k\\ F & F' & k\end{Bmatrix}\sqrt{(2F+1)(2F'+1)(2F_i+1)(2F_i'+1)}(2k+1)$$

and we sum over F_i, F, F_i', F' to obtain the orthonormality relation of the 9j symbols. After rearranging the terms we obtain

$$\frac{\left\langle F_i\ F\left\|I_2^{(0)}\cdot I_1^{(k)}(t)\cdot J^{(0)}\right\|F_i'\ F'\right\rangle}{\left\langle F_i\ F\left\|I_2^{(0)}\cdot I_1^{(0)}\cdot J^{(k)}(0)\right\|F_i'\ F'\right\rangle}=\frac{\left\langle I_1\left\|I_1^{(k)}\right\|I_1\right\rangle\left\langle J\left\|J^{(0)}\right\|J\right\rangle}{\left\langle J\left\|J^{(k)}(0)\right\|J\right\rangle\left\langle I_1\left\|I_1^{(0)}\right\|I_1\right\rangle}$$

$$\times\sum_{F,F'}(2F+1)(2F'+1)(2k+1)^2\sum_{\alpha,\alpha'}\cos\left[\frac{E_{\alpha,F}-E_{\alpha',F'}}{\hbar}\cdot t\right]$$

$$\sum_{F_i,F_i'}C_{F_i\alpha}^{(F)}C_{F_i'a'}^{(F')*}\sqrt{(2F_i+1)(2F_i'+1)}\begin{Bmatrix}I_1 & I_1 & k\\ J & J & 0\\ F_i & F_i' & k\end{Bmatrix}\begin{Bmatrix}I_2 & I_2 & 0\\ F_i & F_i' & k\\ F & F' & k\end{Bmatrix}$$

$$\sum_{F_i'',F_i'''}C_{F_i''\alpha}^{(F)*}C_{F_i'''a'}^{(F')}\sqrt{(2F_i''+1)(2F_i'''+1)}\begin{Bmatrix}I_1 & I_1 & 0\\ J & J & k\\ F_i'' & F_i''' & k\end{Bmatrix}\begin{Bmatrix}I_2 & I_2 & 0\\ F_i'' & F_i''' & k\\ F & F' & k\end{Bmatrix}$$

thus

$$\frac{A_q^k[I_1,t]}{A_q^k[J,0]}=\left(\frac{J(J+1)}{I_1(I_1+1)}\right)^{k/2}\frac{\left\langle I_1\middle\|I_1^{(k)}\middle\|I_1\right\rangle\left\langle J\middle\|J^{(0)}\middle\|J\right\rangle}{\left\langle J\middle\|J^{(k)}(0)\middle\|J\right\rangle\left\langle I_1\middle\|I_1^{(0)}\middle\|I_1\right\rangle}$$
$$\times\sum_{F,F'}(2F+1)(2F'+1)(2k+1)^2\sum_{\alpha,\alpha'}\cos\left[\frac{E_{\alpha,F}-E_{\alpha',F'}}{\hbar}\cdot t\right]$$
$$\sum_{F_i,F_i'}C_{F_i\alpha}^{(F)}C_{F_i'a'}^{(F')*}\sqrt{(2F_i+1)(2F_i'+1)}\begin{Bmatrix}I_1 & I_1 & k\\ J & J & 0\\ F_i & F_i' & k\end{Bmatrix}\begin{Bmatrix}I_2 & I_2 & 0\\ F_i & F_i' & k\\ F & F' & k\end{Bmatrix} \tag{13}$$
$$\sum_{F_i'',F_i'''}C_{F_i''\alpha}^{(F)*}C_{F_i'''a'}^{(F')}\sqrt{(2F_i+1)(2F_i'+1)}\begin{Bmatrix}I_1 & I_1 & 0\\ J & J & k\\ F_i'' & F_i''' & k\end{Bmatrix}\begin{Bmatrix}I_2 & I_2 & 0\\ F_i'' & F_i''' & k\\ F & F' & k\end{Bmatrix}$$

Reducing the 9-j symbols to the corresponding 6-j symbols, we obtain

$$H_{[1]}^{(k)}(I_1,t)=\frac{U_k(I_1)}{U_k(J)}\sum_{F,F'}\frac{(2F+1)(2F'+1)}{(2I_2+1)\sqrt{(2I_1+1)(2J+1)}}\sum_{\alpha\alpha'}\cos\left[\frac{\left(E_{\alpha,F}-E_{\alpha',F'}\right)\cdot t}{\hbar}\right]$$
$$\times\sum_{F_i,F_i'}(-1)^{2F_i'}\sqrt{(2F_i+1)(2F_i'+1)}\;C_{F_i,\alpha}^{(F)}\;C_{F_i',\alpha'}^{(F')*}\begin{Bmatrix}F_i & F_i' & k\\ F' & F & I_2\end{Bmatrix}\begin{Bmatrix}F_i & F_i' & k\\ I_1 & I_1 & J\end{Bmatrix} \tag{14}$$
$$\times\sum_{F_i'',F_i'''}(-1)^{F_i''+F_i'''}\sqrt{(2F_i''+1)(2F_i'''+1)}\;C_{F_i'''\alpha}^{(F')}\;C_{F_i'',\alpha'}^{(F)*}\begin{Bmatrix}F_i'' & F_i''' & k\\ F' & F & I_2\end{Bmatrix}\begin{Bmatrix}F_i'' & F_i''' & k\\ J & J & I_1\end{Bmatrix}$$

where the leading constants have been collected into the ratio $U_k(I_1)/U_k(J)$. Applying the conditions for hierarchical coupling ($C_{F_i,\alpha}^{(F)}=\delta_{F_i,\alpha}$) gives the hierarchical coupling equation for $\mathrm{H}_{[1]}^{(\mathrm{k})}\left(\mathrm{I}_1,\mathrm{t}\right)$

$$H_{[1]}^{(k)}(I_1,t)=\frac{U_k(I_1)}{U_k(J)}\sum_{\substack{F,F'\\F_i,F_i'}}(-1)^{F_i'-F_i}\frac{(2F+1)(2F'+1)(2F_i+1)(2F_i'+1)}{(2I_2+1)\sqrt{(2I_1+1)(2J+1)}}$$
$$\cos\left[\frac{(E_{F_i,F}-E_{F_i',F'})\cdot t}{\hbar}\right]\begin{Bmatrix}F_i & F_i' & k\\ I_1 & I_1 & J\end{Bmatrix}\begin{Bmatrix}F_i & F_i' & k\\ J & J & I_1\end{Bmatrix}\begin{Bmatrix}F_i & F_i' & k\\ F' & F & I_2\end{Bmatrix}^2 \tag{15}$$

In a similar manner, we obtain the following expression for the time-dependence of the polarization of nucleus I_2:

$$\frac{A_q^k[I_2,t]}{A_q^k[J,0]}=\left(\frac{J(J+1)}{I_2(I_2+1)}\right)^{k/2}\frac{\left\langle I_2\left\|I_2^{(k)}\right\|I_2\right\rangle\left\langle J\left\|J^{(0)}\right\|J\right\rangle}{\left\langle J\left\|J^{(k)}(0)\right\|J\right\rangle\left\langle I_2\left\|I_2^{(0)}\right\|I_2\right\rangle}$$
$$\times\sum_{F,F'}(2F+1)(2F'+1)(2k+1)^{3/2}\sum_{\alpha,\alpha'}\cos\left[\frac{E_{\alpha,F}-E_{\alpha',F'}}{\hbar}\cdot t\right]$$
$$\sum_{F_i,F_i'}C_{F_i\alpha}^{(F)}C_{F_i'a'}^{(F')*}\sqrt{(2F_i+1)(2F_i'+1)}\begin{Bmatrix}I_1 & I_1 & 0\\ J & J & 0\\ F_i & F_i' & 0\end{Bmatrix}\begin{Bmatrix}I_2 & I_2 & k\\ F_i & F_i' & 0\\ F & F' & k\end{Bmatrix} \tag{16}$$
$$\sum_{F_i'',F_i'''}C_{F_i''\alpha}^{(F)*}C_{F_i'''a'}^{(F')}\sqrt{(2F_i+1)(2F_i'+1)}\begin{Bmatrix}I_1 & I_1 & 0\\ J & J & k\\ F_i'' & F_i''' & k\end{Bmatrix}\begin{Bmatrix}I_2 & I_2 & 0\\ F_i'' & F_i''' & k\\ F & F' & k\end{Bmatrix}$$

Reducing the 9-j symbols with a vanishing element to 6-j symbols gives, in the general case

$$H_{[2]}^{(k)}(I_2,t)=\frac{U_k(I_2)}{U_k(J)}\sum_{F,F'}\frac{(2F+1)(2F'+1)}{(2I_1+1)\sqrt{(2I_2+1)(2J+1)}}\sum_{\alpha\alpha'}(-1)^{I_1+J+k+F'}\cos\left[\frac{\left(E_{\alpha,F}-E_{\alpha',F'}\right)\cdot t}{\hbar}\right]$$
$$\times\sum_{F_i,F_i'}(-1)^{F_i+F_i'}\sqrt{(2F_i+1)(2F_i'+1)}\;C_{F_i,\alpha}^{(F)}\;C_{F_i',\alpha'}^{(F')*}\begin{Bmatrix}F_i & F_i' & k\\ F' & F & I_2\end{Bmatrix}\begin{Bmatrix}F_i & F_i' & k\\ J & J & I_1\end{Bmatrix} \tag{17}$$
$$\times\sum_{F_i''}(-1)^{3F_i''-F}\;C_{F_i'',\alpha}^{(F')}\;C_{F_i'',\alpha'}^{(F)*}\begin{Bmatrix}F' & F & k\\ I_2 & I_2 & F_i''\end{Bmatrix}$$

whereas applying the conditions for hierarchical coupling ($C_{F_i,\alpha}^{(F)}=\delta_{F_i,\alpha}$) first, and then reducing the 9-j symbols gives the hierarchical coupling description of

$$\mathrm{H}_{[2]}^{(k)}(\mathrm{I}_2,\mathrm{t})=\frac{\mathrm{U_k(I_2)}}{\mathrm{U_k(J)}}\sum_{\mathrm{F,F'}}\sum_{\mathrm{F_i}}(-1)^{(\mathrm{I_1+J+k+F'-F+F_i})}\frac{(2\mathrm{F}+1)(2\mathrm{F}'+1)(2\mathrm{F_i}+1)}{(2\mathrm{I_1}+1)\sqrt{(2\mathrm{I_2}+1)(2\mathrm{J}+1)}}$$
$$\cos\left[\frac{(\mathrm{E_{F_i,F}}-\mathrm{E_{F_i,F'}})\cdot\mathrm{t}}{\hbar}\right]\begin{Bmatrix}\mathrm{F}' & \mathrm{F} & \mathrm{k}\\ \mathrm{I_2} & \mathrm{I_2} & \mathrm{F_i}\end{Bmatrix}\begin{Bmatrix}\mathrm{F}' & \mathrm{F} & \mathrm{k}\\ \mathrm{F_i} & \mathrm{F_i} & \mathrm{I_2}\end{Bmatrix}\begin{Bmatrix}\mathrm{F_i} & \mathrm{F_i} & \mathrm{k}\\ \mathrm{J} & \mathrm{J} & \mathrm{I_1}\end{Bmatrix} \tag{18}$$

In the simplest case where the molecule possesses one or more indistinguishable nuclei, or only one of the nuclei has non zero spin (i.e. I_2=0 and I_1=I), Equation (13) is simplified and the nuclear polarization is described by:

$$H^{(k)}(I,t)=\frac{U_k(I)}{U_k(J)}\sum_{F,F'}(-1)^{F-F'}\frac{(2F+1)(2F'+1)}{\sqrt{(2I+1)(2J+1)}}\cos\left[\frac{(E_F-E_{F'})t}{\hbar}\right]\begin{Bmatrix}F' & F & k\\ J & J & I\end{Bmatrix}\begin{Bmatrix}F' & F & k\\ I & I & J\end{Bmatrix} \tag{19}$$

4. Preparation of highly spin-polarized atoms.

We can now proceed to the main objective of this work, which is to explain how this formalism can be used for the preparation of aligned and oriented atoms. Nuclear spin can be highly polarized from the transfer of molecular rotational polarization via the hyperfine interaction, and on the other hand, large atomic electronic polarization can be produced via molecular photodissociation with polarized light. In combination, these two pulsed-laser techniques can be used to produce highly polarized atoms at densities close to the density of the parent molecules.

d) Systems with one indistinguishable nuclear spin.

We can now proceed to the main objective of this work, which is to explain how this formalism can be used for the preparation of aligned and oriented atoms. Nuclear spin can be highly polarized from the transfer of molecular rotational polarization via the hyperfine interaction, and on the other hand, large atomic electronic polarization can be produced via molecular photodissociation with polarized light. In combination, these two pulsed-laser techniques can be used to produce highly polarized atoms at densities close to the density of the parent molecules.

One of the main initiatives for the development of this method was the search for efficient sources of spin-polarized hydrogen and deuterium atoms where optical pumping is very difficult to be applied due to the lack of continuous ultraviolet laser sources. This method can be used in combination with photodissociation with circularly polarized light in order to surpass the problem of the electron spin depolarization to the nucleus. As explained in the introduction, the electron spin of hydrogen atoms can be polarized to a very large degree via photodissociation of hydrogen – halide molecules with circularly polarized light, but the initial electron

spin polarization is coupled to the proton spin in a sub-nanosecond timescale, decreasing the average electron spin polarization to ½. Thus polarization transfer from molecular rotation to the nuclear spin can be used to outcome this problem. Nevertheless, the method of polarization transfer from molecular rotation to the nuclear spin can be considered as an independent method for the preparation of polarized gasses, since the polarization transfer from the nuclear to the electronic spin is possible.

The easiest way to ensure total polarization transfer from molecular rotation to the proton spin is to choose a system where no other nuclear spins are present. As a first example, consider the H_2 molecule, excited at t=0 to the rovibrational state (v, J=1, m=1) using stimulated Raman pumping. The polarization of J may be described by $A_0^{(1)}(J)=1/\sqrt{2}$ and $A_0^{(2)}(J)=1/2$, (see equation 1a) and detected with Raman scattering [33], whereas the nuclear spin (I=1) is initially unpolarized, $A_0^{(k)}(I)=0$.

We calculate the time-dependence of the m-state distribution (shown in Fig 16) for I and J using equations 9 and 17 for excitation to the J=1 rotational angular momentum state. We see that after about 8 or 10 μs, the initial situation has reversed and now the total nuclear spin I is nearly 100% polarized (and therefore so are both of the individual proton spins), with J now unpolarized. Rapid molecular dissociation at this point (e.g. using VUV or multi-photon or intense laser field dissociation) would produce H atoms or protons that retain this proton polarization. The pulsed optical detection of H atoms has been recently proposed [34]. Complete polarization transfer from J to I may only occur for J=I, with the extent of polarization transfer generally decreasing the more J and I differ in magnitude.

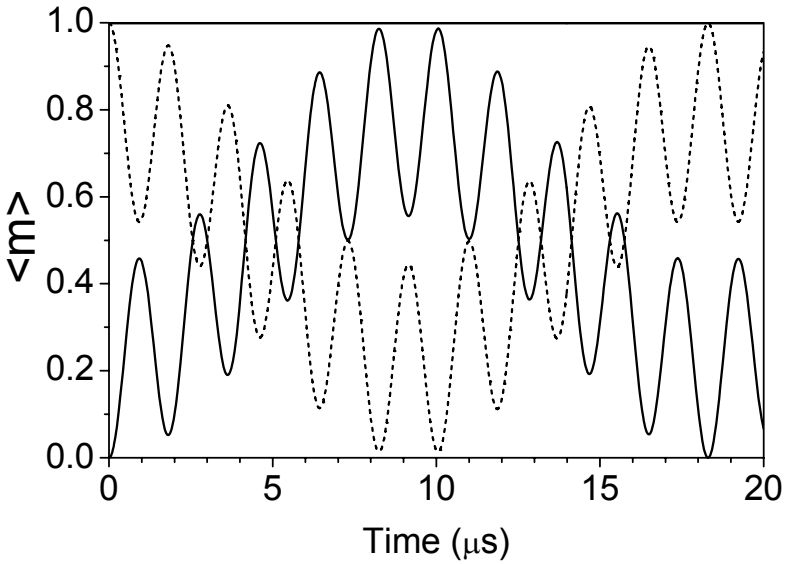

Figure 16: Time dependence of <m> for the proton nuclear spin I=1 (solid line) and the rotational angular momentum J=1 (dotted line) after pulsed preparation of the H_2(v=1,J=1,m=1) state.

Next, consider C_2H_2, excited to the (v, J=1, m=1) state. The calculations show that that the proton spins become nearly 100% polarized ~300 μs after excitation. In contrast to H_2, C_2H_2 may be state-prepared via a one-photon transition, making it a better candidate for optical pumping, and it can be photodissociated readily at 193 nm [35].

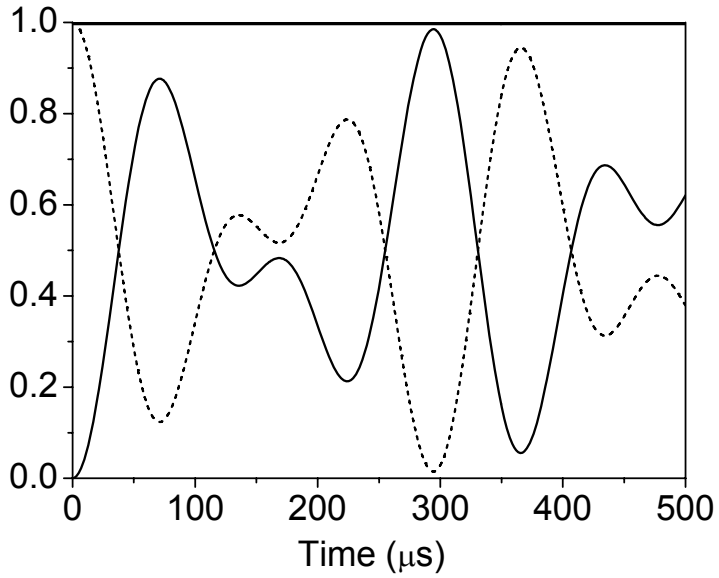

Figure 17: Time dependence of <m> for the proton nuclear spin I=1 (solid line) and the rotational angular momentum J=1 (dotted line) after pulsed preparation of the $C_2H_2(v_i=1,J=1,m=1)$ state.

e) Hydrogen-halide systems.

Next we will consider hydrogen-halide systems. The reason why hydro-halide molecules are considered is because the previously studied systems suffer different problems, as H_2 is difficult to be prepared and dissociated while the polarization transfer in C_2H_2 is slow, a fact that can give rise to experimental difficulties. Additionally, the demonstration of large polarization exhibited in hydro-halide molecules photodissociation, indicates that in such a system those two polarization techniques can be combined if a convenient photodissociation wavelength can be found.

The first system to be examined is $H^{35}Cl$ and its transition from HCl(v=0,J=0) state to HCl(v=1,J=1) state. The electron spin of the chlorine atom can be highly polarized with photodissociation with circularly polarized light [17]. This initial polarization is significantly decreased due to the coupling to the nuclear spin. It is then useful to consider the polarization transfer to the nuclear spin from molecular rotation and to see how it can be useful to overcome the electron spin depolarization problem.

The spin-rotation coupling between J and I_{Cl} is more than two orders of magnitude stronger than that between J and I_H, so the hierarchical coupling expressions may be used to excellent approximation with the hyperfine constants of Kaiser [36]. The time-dependence of $G_{1,2}^{(2)}(J=1,t)$ has been measured by Orr-Ewing et al. [15], and more recently by Lammer et al. [37]for $t \leq 1$ μs. The time-dependence of the m-state distributions for I_H, I_{Cl}, and J is shown in figure 18, as well as their constant sum. At ~145 ns after excitation, $\langle m_{Cl} \rangle$ has increased from 0 to nearly 1.2, and dissociation of the HCl at this time would yield highly polarized ^{35}Cl nuclei. HCl photodissociation at 193nm yields highly *electronically* polarized $^2P_{3/2}$ and $^2P_{1/2}$ Cl atoms. Consequently, combined rovibrational excitation and photodissociation would yield Cl atoms with total projection $\langle m_{Cl} \rangle \approx 1.45$ for $^2P_{1/2}$ and $\langle m_{Cl} \rangle \approx 1.6$ for $^2P_{3/2}$ when averaged over all recoil directions. The extent of polarization could be increased further by photolyzing at shorter wavelengths, for which the electronic polarization is greater [38].

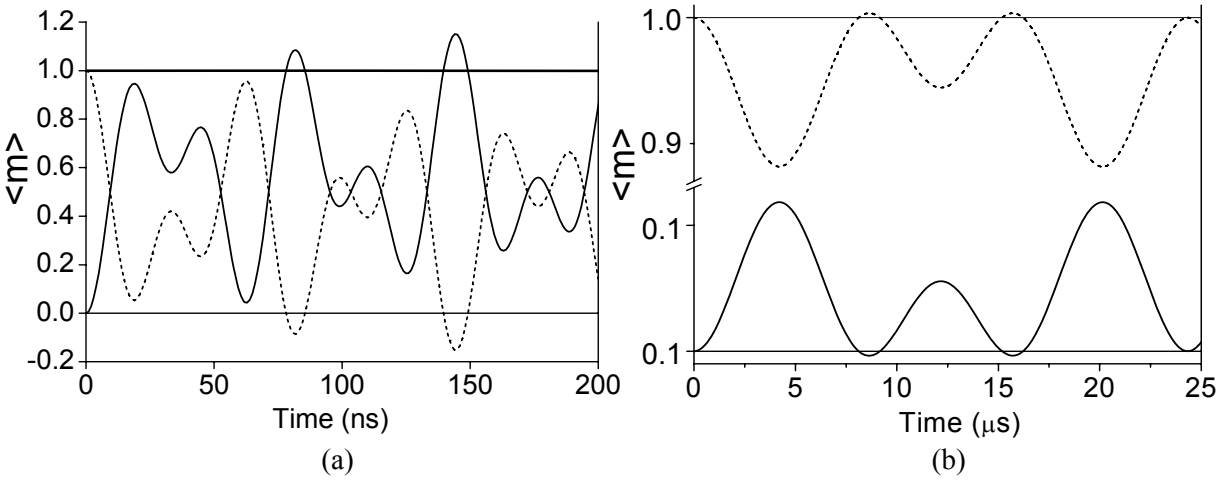

Figure 18: Time dependence of <m> for a) the nuclear spin of ^{35}Cl I_{Cl}=3/2 (solid line) and the rotational angular momentum J=1 (dotted line) after pulsed preparation of the $H^{35}Cl$(v=1,J=1,m=1) state, and b) the nuclear spin of the proton I_H=1/2 (solid line) and the sum of I_{Cl} and J (dotted line).

The time-dependence of the populations of the nuclear m states can be expressed in terms of the $A_0^{(k)}(I,t)$ through equation (1). In the following figure we show how the m-state populations of |m|=3/2 and |m|=1/2 vary with time. At t=0, these populations are each 0.5 (which is the case for unpolarized spins). At about 150 ns, the |m|=1/2 population increases to more than 90%, whereas the complementary |m|=3/2 population decreases to less than 10%. Prompt photodissociation at this point will yield highly aligned ^{35}Cl nuclei; typical photodissociation cross sections are on the order $\sigma_{abs}\approx10^{-18}$ cm^2, so that these transitions can be saturated with commercial pulsed lasers. A second, similar, example is the preparation of H^{35}Cl(v,J=2,m=2) using Raman pumping. In Figure 4b we show the time dependence of the population of the m=+3/2 ^{35}Cl spin state, and also the sum of the remaining 3 nuclear spin states (|m|=1/2 and m=-3/2). At t=0, the ^{35}Cl spin is unpolarized, so each of the 4 m states has a population of 1/4. We see that at about t=32 or 205 ns the populations of the m=+3/2 state has increased to about 90%. Prompt photodissociation at this point will yield highly oriented ^{35}Cl nuclei. These polarized atoms can be used on short timescales, for which the collisional depolarization effects are not significant. On the other hand, the polarization transfer to the proton is predicted to be insignificant. This

is a natural consequence of the system being hierarchical with respect to the chlorine nuclei coupling to the molecular rotation. If we are interested in producing highly spin polarized protons via rotational excitation we have to study systems that are not less accurately by the hierarchical approximation.

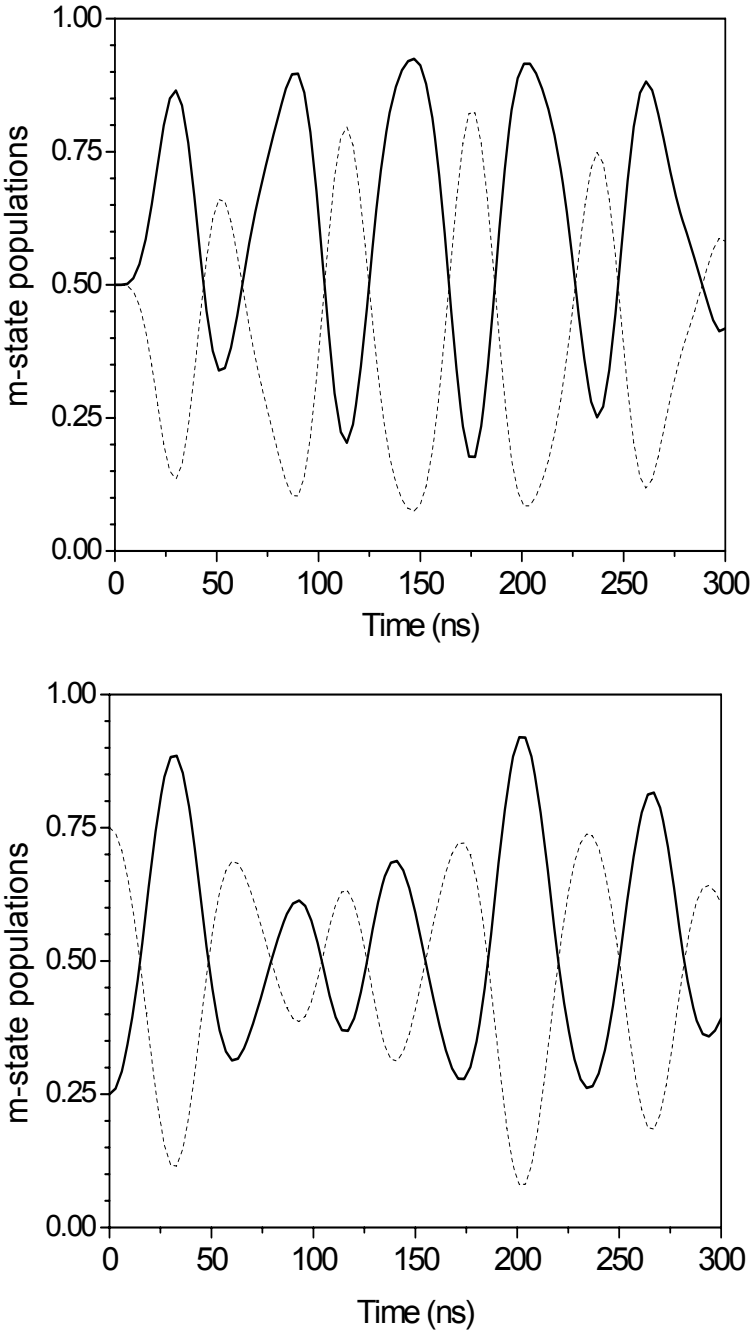

Figure 19: The time-dependence of the m-state populations of the ^{35}Cl nuclear spins in the $H^{35}Cl(v,J)$ molecules following pulsed optical excitation at t=0 from $H^{35}Cl(v=0,J=0)$ for a) the $|m|=1/2$ (solid line) and $|m|=3/2$ (dashed line) states of $H^{35}Cl(v,J=1,m=0)$, and b) the m=3/2 (solid line) and the sum of the $|m|=1/2$ and m=-3/2 states (dashed line) states of $H^{35}Cl(v,J=2,m=2)$.

It should be noted that molecules such as HCl may be cooled in a molecular beam so that most of the population is in the (v=0,J=0) state. Also, it is well within the capabilities of commercially available lasers to saturate both the infrared absorption step, in which HCl is excited to the (v=1,J=1,m=1) state, and the photodissociation step. Furthermore, since the absorption spectrum of the (v=1,J=1) state is shifted significantly to the red with respect to the (v=0,J=0) state, this state may be photodissociated selectively.

Next we examine the well-studied system of HF. We plot the time-dependence of the polarization of J and the H and F nuclear spins (i.e. the $G^{(k)}(J,t)$ and $H_{[i]}^{(k)}(I,t)$ factors) following the prompt preparation of the HF (v=1,J=1,m=1) state. The HF molecule seems to be one of the most promising systems to be used as a source of spin-polarized hydrogen. It is the "less hierarchical" hydrogen-halide system to our knowledge (meaning that the proton hyperfine constant is closer to the halogen constant than every other hydro-halide system), since it is the only one in which the halogen nuclei does not exhibit quadruple coupling to the molecular rotation. Another reason why we study extensively the hydrogen-halide systems is because it has been demonstrated that in these systems the electron spin can be sufficiently polarized via photodissociation with circularly polarized light.

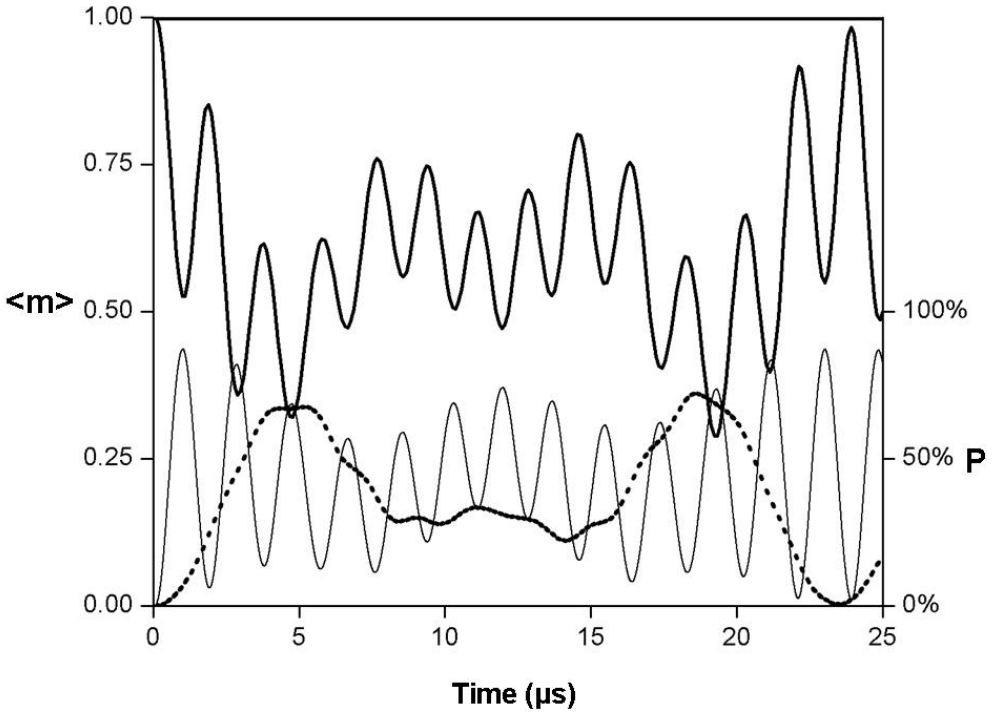

Figure 20: The time-dependence of $\langle m_{J_{HF}} \rangle$ *(bold line),* $\langle m_{I_F} \rangle$ *(solid line) and* $\langle m_{I_H} \rangle$ *(dotted line) as well as their summation (which is always 1), for the prompt preparation of the HF (v=1, J=1, m=1) rovibrational state without hyperfine resolution. Note that all three plots always sum to unity (the initial projection of* m_J*).*

The figure above shows that the values of $H^{(1)}(I_1,t)$ and $H^{(1)}(I_2,t)$ almost reach their maximum values at about 1 and 4 μs. This temporal behavior can be explained by the different values of the hyperfine constants that couple each nuclear spin to the molecular rotation. In the HF molecule in particular the ratio of these constants is $C_F/C_H \sim 5.3$ (for v = J = 1), and this situation has an approximate correspondence to the relative frequencies of the nuclear polarization beatings. It should be noted here that if the time-averaged polarization of the nuclear spins is detected, instead of the maximum nuclear polarizations that can be obtained at specific times, the polarization obtained is going to be much smaller. For the situation presented here, the average molecular depolarization and corresponding nuclear polarization will be $\langle m_J \rangle$ = 0.596, $\langle m_{I_F} \rangle$ = 0.213, and $\langle m_{I_H} \rangle$ = 0.191. The average depolarization and polarization values satisfy conservation of angular momentum projection. Application

of the hierarchical approximation give slightly smoother plots for the polarization factor, and as explain previously fail at very large times.

f) Deuterium-halide systems.

The previous examples show that preparation of spin polarized hydrogen atoms via polarization transfer although promising is not trivial. The 100% polarization transfer exhibited in systems where protons are the only nuclear spins present is difficult to be exploited since neither it occurs in very large times as in the case of C_2H_2 or the photodissociation wavelengths are difficult to be found as in the case of H_2. On the other hand, hydro-halide molecules are easily dissociated with current dye-lasers the polarization transfer though is usually dominated by the halide nucleus, especially when quadrupolic interaction is present. The fact that the fluorine nucleus has spin of only ½ makes it perhaps the best candidate among the hydro-halide molecules. Even in this case though the polarization transfer is mostly dominated by the halogen nucleus and a significant amount of time has to pass until the proton is significantly polarized.

This situation is expected to be different when the proton is replaced by deuterium in the cases were the quadrupole coupling that deuterium exhibits suffices to inverse the situation and to make deuterium the strongly coupled nucleus. This of course is not the case for DCl, since as we discussed in the previous chapter, the presence of quadrupole term in the deuterium nucleus coupling hardly alters the depolarization time-dependence with respect to the one for HCl. Of course deuterium acquires higher degree of polarization than the proton in HCl, but again, the dominant polarization transfer occurs between J and the chlorine nucleus.

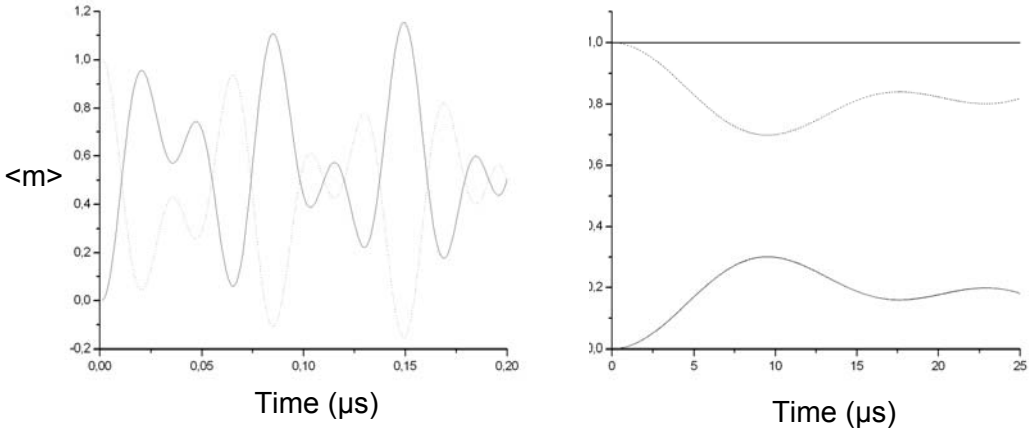

Figure 21: The time-dependence of <m> for molecular rotation and chlorine nuclear spin (left) as well as the summation of these two shown with <m> of the deuterium nuclear spin for a larger time interval. Note that all three plots always sum to unity (the initial projection of m_I).

The situation is reversed in the case of DF, since now the nuclear spin of deuterium is the largest one in the system. The coupling between molecular rotation and the fluorine nucleus remains important so none of the two nuclei can be considered to couple preferentially to J so that the hierarchical approximation can used. We plot the time dependence of the angular momentum projections for the case of the pulsed excitation of the (v=0, J=1, m=1) state of DF. We note that D nuclei with $\langle m_D \rangle \approx 0.6$ can be produced by exciting the (v=0, J=1, m=1) state of DF, and by photodissociating after about 4.5 μs, while an even bigger value of $\langle m_D \rangle \approx 0.7$ is achieved after 15 μs. The polarization transfer to the fluorine nucleus is small since $\langle m_F \rangle$ is always smaller than 0.3.

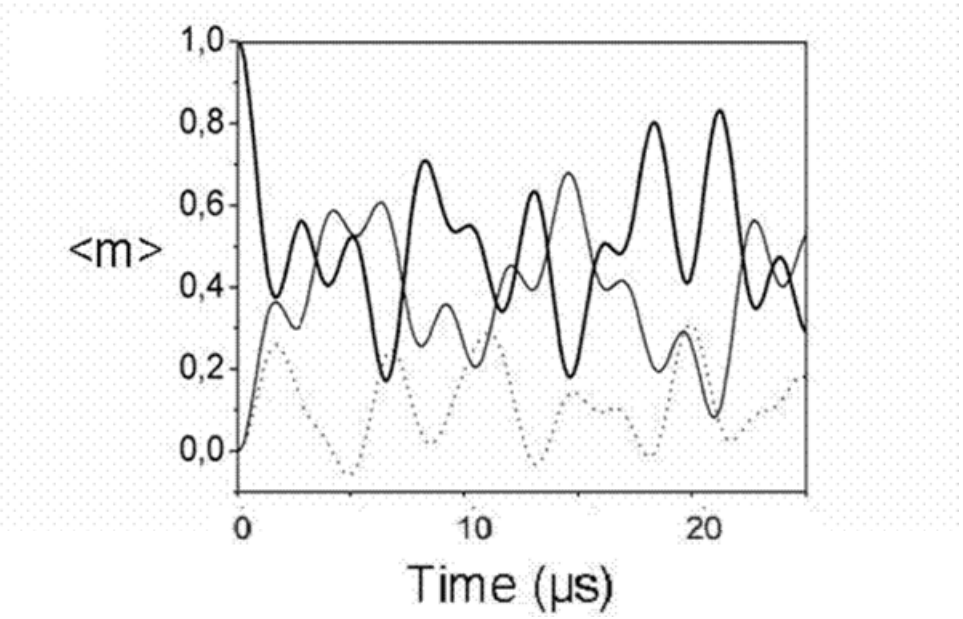

Figure 22: The time-dependence of $\langle m_{J_{DF}} \rangle$ *(bold line),* $\langle m_{I_D} \rangle$ *(solid line) and* $\langle m_{I_F} \rangle$ *(dotted line) as well as their summation (which is always 1), for the prompt preparation of the DF (v=0, J=1, m=1) rovibrational state without hyperfine resolution, for calculations using the nonhierarchical coupling expressions.*

(D) Conclusions.

We have shown when optical excitation occurs in composite angular momentum systems such as molecules, and the bandwidth of the radiation used is such that the procedure occurs without hyperfine resolution, the interaction of the initially polarized molecular rotation with the randomly distributed nuclear spins results to a temporal beating of the alignment (or orientation) so that the orientation or alignment of the molecular rotation is decreased. A similar situation is observed when an atom's electronic spin is polarized via photodissociation or any other prompt procedure and the polarization is reduced due to its coupling to the nuclear spin.

Although this situation is considered a drawback when optical excitation is considered for the preparation of polarized molecules, it provides with the unique possibility to polarize the indirectly an atom's nuclear spin. Since the molecular depolarization coefficient $G^k(J,t)$ as well as the nuclear spin polarization coefficients $H^{(k)}_{[1,2]}(I_{1,2},t)$ can be calculated form angular momentum theory, the polarization transfer form the molecular rotation to the nuclear spin and back, can be predicted and thus the appropriate time can be found when by photodissociating the molecule the procedure is "frozen", and the produced fragments are selectively polarized. This new polarization concept can be combined with the technique of polarizing atoms via molecular photodissociation with circularly polarized light [14,21], or it can be used as an independent technique.

The equations needed are developed in the framework of the $A^{(k)}_q(J)$ multiple moment representation of an angular momentum distribution but it is easy to perform the transformation to the density matrix representation if necessary. In general these equations are obtained with the use of the Wigner-Eckart theorem and other useful theorems of quantum angular momentum. For systems where one nuclear spin is much more strongly coupled to the molecular rotation than the other (for example due to the presence of quadrupolic coupling to one of them), the hierarchical coupling approximation can be imposed and significantly simplified equations can be produced. The situation where the molecule contains one indistinguishable nuclear spin is treated though even more simplified expressions.

There are many situations where such a procedure can be used for the preparation of highly polarized halide atoms, to be used for example in chemical dynamics studies as polarized reagents. In hydrogen-halide molecules the halide nucleus usually dominates the polarization transfer and significant polarization can be achieved within times in the order of microseconds. The preparation of polarized hydrogen atoms through this technique is less trivial, since we need to consider systems in which a high degree of polarization is transferred to the proton spin and the excitation and dissociation steps do not exhibit big difficulties.

The main initiative for the development of this technique was the search for polarized hydrogen atoms sources, since due to the large energetic distance between the first two levels of hydrogen atoms (10.2eV corresponding to 121nm excitation wavelength), is such that optical pumping cannot be applied. For systems with one indistinguishable nuclear spin such as H_2 or C_2H_2, the proton spin can be found to be 100% polarized. Unfortunately both these choices turn to exhibit serious drawbacks since on the one hand H_2 can be photodissociated only with XUV radiation or multiphoton dissociation while polarization transfer in C_2H_2 on the other hand occurs in very large times, a fact that could impose big experimental difficulties.

The hydro-halide molecules are much more promising as potential sources of polarized sources, especially since large degree of polarization is demonstrated to be obtained via photodissociation with circularly polarized light. Furthermore, in such a procedure the electronic spin is coupled to nuclear spin. Combination of these two techniques can lead to even higher degrees of polarization, since the electronic and the nuclear spin can be independently polarized. However, for this direction to be explored, appropriate optical excitation schemes must be found (such as vibrational or electronic excitation), and the photofragment polarization from the photodissociation of these excited states must be quantified. Here we analyze excitation of HF molecule and we show that significant polarization (~80%) can be produced within approximately 5 microseconds.

The task of polarizing deuterium's nuclear spin, which would exhibit more or less the same difficulty if optical pumping was considered, is proved here to be easier. This is especially due to the deuterium dominating the angular momentum transfer that follows excitation of DF to the v = 1, J = 1 rovibrational state. There deuterium spin can be polarized up to 60% in times smaller than 10 microseconds.

The method of polarizing the nuclear spin via the hyperfine interaction along

with the method of polarizing the electron spin via photodissociation look both very good candidates for high density polarized gases preparation. The present technique seems to be dependent both on the photodissociation and the optical excitation cross-sections. Furthermore, since the photodissociation step is, in many circumstances selective with respect to the rotational state, the population that "escaped" the excitation state is not observed. Furthermore, the density achievable is close to the density of the parent molecule, and can exceed 10^{16} atoms/cm^3, which are orders of magnitude larger than existing techniques.

APPENDIX (1). *Calculation of the eigenenergies* $E_{F_i,\alpha}$ *and eigenvectors* $C^{(F)}_{F_i,\alpha}$ **.**

The information available from experimental measurements such as [Breant, Kaiser,Muenter,etc] for the hyperfine Hamiltonian structure are not directly used in the description of the polarization transfer from molecular rotation to the nuclear spin, since a series of transformations is required in order to produce the eigenenergies $E_{F_i,\alpha}$ and eigenvectors $C^{(F)}_{F_i,\alpha}$ needed**.** . In this appendix a simple method for producing $E_{F_i,\alpha}$ and $C^{(F)}_{F_i,\alpha}$ is presented and an example of the code that generates the various plots presented in the document is given.

The energy dependence of the formulas produced here comes from the evaluation of the reduced matrix elements $\left\langle F_i F \left\| e^{\frac{iHt}{t}} \right\| F_i' F \right\rangle$ which are obtained after expressing the time dependence of the tensor operator $T^{(k)}(t)$ in the Heisenberg interaction picture. The substitution $\frac{\left\langle F_i F \left\| e^{\frac{iHt}{t}} \right\| F_i' F \right\rangle}{\sqrt{2F+1}} = \sum_{\alpha} C^{(F)}_{F_i,\alpha} e^{i\frac{Et}{\hbar}} C^{(F)*}_{F_i',\alpha'}$ means that the time dependence of the reduced matrix element can be calculated in the appropriate basis .The hyperfine Hamiltonian is expressed initially in the uncoupled representation and its dimension is $(2J+1)(2I_1+1)(2I_2+1)^2$. It can be directly evaluated in this representation, since the products of the form $I_1 I_2$ can be analyzed with the use of the ladder operators as since $I_i = ½(I_{i+} + I_{i-}) + I_{iz.}$ On the other hand, our system is depended in the total angular momentum F and the intermediate coupling quantum number Fi, so the hyperfine Hamiltonian in the uncoupled representation is expected to exhibit degeneracy.

The way to express the Hamiltonian in the coupled representation is to evaluate it in the coupled basis. For the general case of a molecule consisted form two distinct nuclei is:

$$\left| I_2 (I_1 J) F_i, F M_F \right\rangle = \sum_{\substack{m_1, m_2, m_3, \\ M_{F_i}}} \left\langle I_1\, m_1, J\, m_J \left| F_i\, M_{F_i} \right\rangle \left\langle I_2\, m_2, F_i\, M_{F_i} \right| F\, M_F \right\rangle \left| I_1\, m_1 \right\rangle \left| I_2\, m_2 \right\rangle \left| J\, m_J \right\rangle$$

Thus the passage form the couple to the uncoupled representation is done simply by

$$\left\langle I_2(I_1J)F_i',F'M'_F\left|H\right|I_2(I_1J)F_i,FM_F\right\rangle=\sum_{\substack{m_1,m_2,m_J,\\ M_{F_i}M_F\\ m_1',m_2',m_J',\\ M_{F_i}'M_F'}}\left\langle I_1\,m_1,J\,m_J\left|F_i\,M_{F_i}\right\rangle\right\langle I_2\,m_2,F_i\,M_{F_i}\left|F\,M_F\right\rangle$$
$$\times\left\langle I_1\,m_1',J\,m_J'\left|F_i'M_{F_i'}\right\rangle\right\langle I_2\,m_2',F_i'M_{F_i'}\left|F'M_{F'}\right\rangle$$
$$\times\left\langle I_1\,m_1\left|\left\langle I_2\,m_2\left|\left\langle J\,m_J\left|H\right|I_1\,m_1\right\rangle\right|I_2\,m_2\right\rangle\right|J\,m_J\right\rangle$$

If we constrain here the values of M_F, M_{Fi}, $M_{F'}$, $M_{Fi'}$ to the values allowed form the angular momentum transition rules ($M_{F_i}=m_J+m_{I_1}, M_F=m_{F_i}+m_{I_2}$) the dimensionality is decreased to the point that there is no degeneracy in the coupled basis Hamiltonian matrix.

The final step is to diagonalize the Hamiltonian to obtain the eigenenergies $E_{F_i,\alpha}$ and eigenvectors $C^{(F)}_{F_i,\alpha}$ needed. In the limit of the hierarchical approximation, the coupled Hamiltonian is already diagonal and this step is unnecessary, the eigenvectors $C^{(F)}_{F_i,\alpha}$ are either unity or one. Such a situation does not exist, since each of the nuclei is coupled to the rotational angular momentum independently. On the other hand, if we have already followed this procedure to produce the Hamiltonian matrix in the coupled basis, there's no need in using the hierarchical formalism any more, since this is the only extra step required for the exact solution. Practically, when the hyperfine constants of the nuclei involved are very different, so that the hierarchical approximation is justified there are more easy ways in obtaining the necessary energies. One of them is to construct and evaluate the hyperfine Hamiltonian matrix and to evaluate it numerically. Diagonalization of this matrix will produce the desired energies with degeneracy, and we have only to include each of the energies once. One other way is to calculate the energies by considering the cross term $I_1*I_2 \sim 0$.In this case the energies terms proportional to I_1J and I_2*J are substituted by $I_1J = ½(F_i(F_i+1)-I_1(I_1+1)-J(J+1))$ and
$I_2J = ½(F(F+1)-F_i(F_i+1)-I_2(I_2+1))$, the nuclear spin operator are considered to conjugate with J and the Hamiltonian is calculated straightforwardly. We note here that in the plots where the hierarchical approximation is compared to the exact solution we do not make use of these options and the differences between the two solutions are generated by the eigenvectors $C^{(F)}_{F_i,\alpha}$. On the other hand, in systems where the hierarchical approximation is valid calculation of the energies with one of the approximating ways mentioned above does not alter the plots significantly.

APPENDIX (2). ***An example of the code (in Mathematica), used in the evaluation of*** $G^k(J,t)$ ***and*** $H^{(k)}_{[1,2]}(I_{1,2},t)$**.**

```
"In this file we construct the Hamiltonian matrix Ham by
spanning our Hamiltonian [39] into ladder operators, expressed
via the function HOP. To check our result we construct the
matrix Ham and diagonalize it. The eigenvalues are degenerate
as expected, and the values are the same of the ones obtained
when one diagonalize the Hamiltonian of Weiss [40], thus the
two Hamiltonians are equivalent.";
Clear[J, I1, I2, V];
J = 1;
I1 = 1/2;
I2 = 1/2;
V = 1;
"Give values for hyperfine coupling constants.(experimental Table 2)(kHz?)";
CF0 = 308.1*10^3; aF = 53*10^3; bF = 0.17*10^3;
CH0 = -70.1*10^3; aH = 1.99*10^3; bH = 0.036*10^3;
SHF0 = 28.7*10^3; aHF = -1*10^3;
CHF = 0*10^3;
"Define each coupling term In*Im to make the HOP function more transparent";
I1J[mj_, m1_, m2_, mjp_, m1p_, m2p_] :=
  (1/2 * Sqrt[(I1*(I1+1) - m1p*(m1p+1))] * KroneckerDelta[m1, m1p+1] * KroneckerDelta[m2, m2p] *
     Sqrt[(J*(J+1) - mjp*(mjp-1))] * KroneckerDelta[mj, mjp-1]
   + 1/2 * Sqrt[(I1*(I1+1) - m1p*(m1p-1))] * KroneckerDelta[m1, m1p-1] * KroneckerDelta[m2, m2p] *
     Sqrt[(J*(J+1) - mjp*(mjp+1))] * KroneckerDelta[mj, mjp+1]
   + m1p * KroneckerDelta[m1, m1p] * KroneckerDelta[m2, m2p] * mjp * KroneckerDelta[mj, mjp]);
I2J[mj_, m1_, m2_, mjp_, m1p_, m2p_] :=
  (1/2 * KroneckerDelta[m1, m1p] * Sqrt[(I2*(I2+1) - m2p*(m2p+1))] * KroneckerDelta[m2, m2p+1] *
     Sqrt[(J*(J+1) - mjp*(mjp-1))] * KroneckerDelta[mj, mjp-1]
   + 1/2 * KroneckerDelta[m1, m1p] * Sqrt[(I2*(I2+1) - m2p*(m2p-1))] * KroneckerDelta[m2, m2p-1] *
     Sqrt[(J*(J+1) - mjp*(mjp+1))] * KroneckerDelta[mj, mjp+1]
   + KroneckerDelta[m1, m1p] * m2p * KroneckerDelta[m2, m2p] * mjp * KroneckerDelta[mj, mjp]);
```

```
I2I1[mj_, m1_, m2_, mjp_, m1p_, m2p_] :=
 (1/2 * √(I1 * (I1 + 1) - m1p * (m1p + 1)) * KroneckerDelta[m1, m1p + 1]
    * √(I2 * (I2 + 1) - m2p * (m2p - 1)) * KroneckerDelta[m2, m2p - 1] * KroneckerDelta[mj, mjp]
   + 1/2 * √(I1 * (I1 + 1) - m1p * (m1p - 1)) * KroneckerDelta[m1, m1p - 1]
    * √(I2 * (I2 + 1) - m2p * (m2p + 1)) * KroneckerDelta[m2, m2p + 1] * KroneckerDelta[mj, mjp]
   + m1p * KroneckerDelta[m1, m1p] * m2p * KroneckerDelta[m2, m2p] * KroneckerDelta[mj, mjp]);

I2JI1J[mj_, m1_, m2_, mjp_, m1p_, m2p_] :=
 (1/4 * √(I1 * (I1 + 1) - m1p * (m1p + 1)) * KroneckerDelta[m1, m1p + 1] * √(I2 * (I2 + 1) - m2p * (m2p + 1)) *
    KroneckerDelta[m2, m2p + 1] * √(J * (J + 1) - mjp * (mjp - 1)) * √(J * (J + 1) - (mjp - 1) * (mjp - 2)) *
    KroneckerDelta[mj, mjp - 2] +
  1/4 * √(I1 * (I1 + 1) - m1p * (m1p + 1)) * KroneckerDelta[m1, m1p + 1] * √(I2 * (I2 + 1) - m2p * (m2p - 1)) *
    KroneckerDelta[m2, m2p - 1] * √(J * (J + 1) - mjp * (mjp + 1)) * √(J * (J + 1) - mjp * (mjp + 1)) *
    KroneckerDelta[mj, mjp] +
  1/4 * √(I1 * (I1 + 1) - m1p * (m1p - 1)) * KroneckerDelta[m1, m1p - 1] * √(I2 * (I2 + 1) - m2p * (m2p + 1)) *
    KroneckerDelta[m2, m2p + 1] * √(J * (J + 1) - mjp * (mjp - 1)) * √(J * (J + 1) - mjp * (mjp - 1)) *
    KroneckerDelta[mj, mjp] +
  1/4 * √(I1 * (I1 + 1) - m1p * (m1p - 1)) * KroneckerDelta[m1, m1p - 1] * √(I2 * (I2 + 1) - m2p * (m2p - 1)) *
    KroneckerDelta[m2, m2p - 1] * √(J * (J + 1) - mjp * (mjp + 1)) * √(J * (J + 1) - (mjp + 1) * (mjp + 2)) *
    KroneckerDelta[mj, mjp + 2] +
  1/2 * mjp * m2p * KroneckerDelta[m2, m2p] * √(J * (J + 1) - mjp * (mjp - 1)) * KroneckerDelta[mj, mjp - 1] *
    √(I1 * (I1 + 1) - m1p * (m1p + 1)) * KroneckerDelta[m1, m1p + 1] +
  1/2 * mjp * m2p * KroneckerDelta[m2, m2p] * √(J * (J + 1) - mjp * (mjp + 1)) * KroneckerDelta[mj, mjp + 1] *
    √(I1 * (I1 + 1) - m1p * (m1p - 1)) * KroneckerDelta[m1, m1p - 1] +
  1/2 * √(J * (J + 1) - mjp * (mjp - 1)) * KroneckerDelta[mj, mjp - 1] * √(I2 * (I2 + 1) - m2p * (m2p + 1)) *
    KroneckerDelta[m2, m2p + 1] * (mjp - 1) * m1p * KroneckerDelta[m1, m1p] +
  1/2 * √(J * (J + 1) - mjp * (mjp + 1)) * KroneckerDelta[mj, mjp + 1] * √(I2 * (I2 + 1) - m2p * (m2p - 1)) *
    KroneckerDelta[m2, m2p - 1] * (mjp + 1) * m1p * KroneckerDelta[m1, m1p] +
  mjp^2 * KroneckerDelta[mj, mjp] * m1p * KroneckerDelta[m1, m1p] * m2p * KroneckerDelta[m2, m2p]);
```

```
I1JI2J[mj_, m1_, m2_, mjp_, m1p_, m2p_] :=
  (1/4 * Sqrt[I2*(I2+1) - m2p*(m2p+1)] * KroneckerDelta[m2, m2p+1] * Sqrt[I1*(I1+1) - m1p*(m1p+1)] *
    KroneckerDelta[m1, m1p+1] * Sqrt[J*(J+1) - mjp*(mjp-1)] * Sqrt[J*(J+1) - (mjp-1)*(mjp-2)] *
    KroneckerDelta[mj, mjp-2] +
   1/4 * Sqrt[I2*(I2+1) - m2p*(m2p+1)] * KroneckerDelta[m2, m2p+1] * Sqrt[I1*(I1+1) - m1p*(m1p-1)] *
    KroneckerDelta[m1, m1p-1] * Sqrt[J*(J+1) - mjp*(mjp+1)] * Sqrt[J*(J+1) - mjp*(mjp+1)] *
    KroneckerDelta[mj, mjp] +
   1/4 * Sqrt[I2*(I2+1) - m2p*(m2p-1)] * KroneckerDelta[m2, m2p-1] * Sqrt[I1*(I1+1) - m1p*(m1p+1)] *
    KroneckerDelta[m1, m1p+1] * Sqrt[J*(J+1) - mjp*(mjp-1)] * Sqrt[J*(J+1) - mjp*(mjp-1)] *
    KroneckerDelta[mj, mjp] +
   1/4 * Sqrt[I2*(I2+1) - m2p*(m2p-1)] * KroneckerDelta[m2, m2p-1] * Sqrt[I1*(I1+1) - m1p*(m1p-1)] *
    KroneckerDelta[m1, m1p-1] * Sqrt[J*(J+1) - mjp*(mjp+1)] * Sqrt[J*(J+1) - (mjp+1)*(mjp+2)] *
    KroneckerDelta[mj, mjp+2] +
   1/2 * mjp * m1p * KroneckerDelta[m1, m1p] * Sqrt[J*(J+1) - mjp*(mjp-1)] * KroneckerDelta[mj, mjp-1] *
    Sqrt[I2*(I2+1) - m2p*(m2p+1)] * KroneckerDelta[m2, m2p+1] +
   1/2 * mjp * m1p * KroneckerDelta[m1, m1p] * Sqrt[J*(J+1) - mjp*(mjp+1)] * KroneckerDelta[mj, mjp+1] *
    Sqrt[I2*(I2+1) - m2p*(m2p-1)] * KroneckerDelta[m2, m2p-1] +
   1/2 * Sqrt[J*(J+1) - mjp*(mjp-1)] * KroneckerDelta[mj, mjp-1] * Sqrt[I1*(I1+1) - m1p*(m1p+1)] *
    KroneckerDelta[m1, m1p+1] * (mjp-1) * m2p * KroneckerDelta[m2, m2p] +
   1/2 * Sqrt[J*(J+1) - mjp*(mjp+1)] * KroneckerDelta[mj, mjp+1] * Sqrt[I1*(I1+1) - m1p*(m1p-1)] *
    KroneckerDelta[m1, m1p-1] * (mjp+1) * m2p * KroneckerDelta[m2, m2p] +
   m1p * m2p * mjp^2 * KroneckerDelta[m1, m1p] * KroneckerDelta[m2, m2p] * KroneckerDelta[mj, mjp]);

"Evaluate HOP function ";
Clear[HOP];

HOP[mj_,m1_,m2_,mjp_,m1p_,m2p_]:=
    CF*I1J[mj,m1,m2,mjp,m1p,m2p]+
      CH*I2J[mj,m1,m2,mjp,m1p,m2p]+
                  CHF*I2I1[mj,m1,m2,mjp,m1p,m2p]+(SHF)/((2*J+3)*(2*J-
1))*(3*I1JI2J[mj,m1,m2,mjp,m1p,m2p]+3*I2JI1J[mj,m1,m2,mjp,m1p,m2p]-
2*J*(J+1)*I2I1[mj,m1,m2,mjp,m1p,m2p]);

Clear[Ham,q];Ham={};q=0;
Do[
```

```
Do[
 Do[AppendTo[Ham,{}];q++;
  Do[
   Do[
    Do[AppendTo[Ham[[q]],HOP[mj,m1,m2,mjp,m1p,m2p]]
     ,{m2p,I2,-I2,-1}]
    ,{m1p,I1,-I1,-1}]
   ,{mjp,J,-J,-1}]
  ,{m2,I2,-I2,-1}]
 ,{m1,I1,-I1,-1}]
,{mj,J,-J,-1}]
```

```
"That's our Hamiltonian in the uncoupled representation";
Ham//MatrixForm
```

$$\begin{pmatrix}
149471. & 0 & 0 & 0 & 0 & 0 & 0 & 0 & 0 & 0 & 0 & 0 \\
0 & 211969. & -2770. & 0 & -42234.1 & 0 & 0 & 0 & 0 & 0 & 0 & 0 \\
0 & -2770. & -217509. & 0 & 261453. & 0 & 0 & 0 & 0 & 0 & 0 & 0 \\
0 & 0 & 0 & -143931. & 0 & 249701. & -53986.2 & 0 & 16620. & 0 & 0 & 0 \\
0 & -42234.1 & 261453. & 0 & -5540. & 0 & 0 & 0 & 0 & 0 & 0 & 0 \\
0 & 0 & 0 & 249701. & 0 & 5540. & 5540. & 0 & -53986.2 & 0 & 0 & 0 \\
0 & 0 & 0 & -53986.2 & 0 & 5540. & 5540. & 0 & 249701. & 0 & 0 & 0 \\
0 & 0 & 0 & 0 & 0 & 0 & 0 & -5540. & 0 & 261453. & -42234.1 & 0 \\
0 & 0 & 0 & 16620. & 0 & -53986.2 & 249701. & 0 & -143931. & 0 & 0 & 0 \\
0 & 0 & 0 & 0 & 0 & 0 & 0 & 261453. & 0 & -217509. & -2770. & 0 \\
0 & 0 & 0 & 0 & 0 & 0 & 0 & -42234.1 & 0 & -2770. & 211969. & 0 \\
0 & 0 & 0 & 0 & 0 & 0 & 0 & 0 & 0 & 0 & 0 & 149471.
\end{pmatrix}$$

```
"This is to check Hermicity";
Clear[k]; k = 0;
Do[
  Do[Clear[t]; t = ( Ham[[i]][[j]] - Ham[[j]][[i]]);
   If[SetAccuracy[t, 6] == 0, k++,
    Print[i]; Print[" ", j]; Print["***ERROR***", t]], {i, 1, Length[Ham]}], {j, 1, Length[Ham]}];
If[k == Length[Ham]^2, Print["Everything is COOL! the matrix is hermitian"]]
```

"...and these are the eigenvalues, which should correspond to the hierarchical energies";

Eigenvalues[Ham]//MatrixForm

$$\begin{pmatrix} -394393. \\ -394393. \\ -394393. \\ -265702. \\ 233842. \\ 233842. \\ 233842. \\ 149471. \\ 149471. \\ 149471. \\ 149471. \\ 149471. \end{pmatrix}$$

```
"this is the Base TRansformation function connecting |m1,m2,mj> states to |Fi,F,mF> states. ";
Clear[BTR];
BTR[F_, Fi_, Fp_, Fip_] :=
  Sum[
   Sum[
    Sum[
     Sum[
      Sum[
       Sum[
        Clear[mi, mip, mfp, mf];
        mi = m1 + mj;
        mip = m1p + mjp;
        mf = mi + m2;
        mfp = mip + m2p;
        (-1)^(2*(I1+I2-J)-Fi-Fip+mf+mfp+mi+mip) *
         Sqrt[(2*F+1)*(2*Fp+1)*(2*Fi+1)*(2*Fip+1)] *
         ThreeJSymbol[{I1, m1p}, {J, mjp}, {Fip, -mip}] *
         ThreeJSymbol[{I2, m2p}, {Fip, mip}, {Fp, -mfp}] *
         ThreeJSymbol[{I2, m2}, {Fi, mi}, {F, -mf}] *
         ThreeJSymbol[{I1, m1}, {J, mj}, {Fi, -mi}] *
         HOP[mj, m1, m2, mjp, m1p, m2p]
        , {mjp, J, -J, -1}]
       , {m1p, I1, -I1, -1}]
      , {m2p, I2, -I2, -1}]
     , {mj, J, -J, -1}]
    , {m1, I1, -I1, -1}]
   , {m2, I2, -I2, -1}];
```

"Here we generate the Matrix itself...Notice the use of chop to avoid problems when sorting the eigenvectors";

```
Clear[Ham2,q];q=0;Ham2={};
Do[
  Do[AppendTo[Ham2,{}];q++;
   Do[
    Do[AppendTo[Ham2[[q]],Chop[BTR[F,Fi,Fp,Fip],8]]
     ,{Fp,Abs[Fip+I2],Abs[Fip-I2],-1}],{Fip,Abs[J+I1],Abs[J-I1],-
1}],{F,Abs[Fi+I2],Abs[Fi-I2],-1}],{Fi,Abs[J+I1],Abs[J-I1],-1}];
```

"this is the matrix";

Ham2//MatrixForm

$$\begin{pmatrix} 747355. & 0 & 0 & 0 \\ 0 & 698405. & 76633.4 & 0 \\ 0 & 76633.4 & -1.18006\times 10^{6} & 0 \\ 0 & 0 & 0 & -265702. \end{pmatrix}$$

"This matrix is constructed in the F,Fi bases. We are going to need those states so we are constructing them simply as the 'pure' states of this system";

```
Clear[Fist,l];
Clear[flag];flag=0;
Do[
  Do[++flag;l={};

Do[If[flag  i,AppendTo[l,1],AppendTo[l,0]],{i,1,Length[Ham2]}];Fist[F][Fi]=l;Clear[l]
   ,{F,Abs[Fi+I2],Abs[Fi-I2],-1}]
  ,{Fi,Abs[J+I1],Abs[J-I1],-1}];
Clear[FLIST];FLIST={};
Do[
 Do[
  AppendTo[FLIST,Fist[F][Fi]]
  ,{F,Abs[Fi+I2],Abs[Fi-I2],-1}]
 ,{Fi,Abs[J+I1],Abs[J-I1],-1}]
```

"These are the eigenvectors of Ham2";

Eigenvectors[Ham2]//MatrixForm

$$\begin{pmatrix} 0. & -0.0406944 & 0.999172 & 0. \\ 1. & 0. & 0. & 0. \\ 0. & 0.999172 & 0.0406944 & 0. \\ 0. & 0. & 0. & 1. \end{pmatrix}$$

"Here I construct the alpha states. They really are the eigenvectors of Ham2.The problem comes in assigning them with a quantum number F,Fi. Now I can 'guess', and that's what I am really doing, since the system is almost hierarchical so the energies are close to those of |F,Fi> states, but I don't know how to do it for a system that's purely non hierarchical. Unfortunately I cannot come up with a systematic method. Notice that for the program not to crush we have to define the non existing Alpha states as zeros.";

```
Clear[Alpha];
Alpha[J +I1+I2][J +I1]=Sum[Eigenvectors[Ham2][[2]]*FLIST[[i]],{i,1,Length[Ham2]}];
Alpha[J +I1+I2][J -I1]={0,0,0,0};
Alpha[J -I1-I2][J +I1]={0,0,0,0};
Alpha[J +I1-I2][J +I1]=Sum[Eigenvectors[Ham2][[3]]*FLIST[[i]],{i,1,Length[Ham2]}];
Alpha[J -I1+I2][J -I1]=Sum[Eigenvectors[Ham2][[1]]*FLIST[[i]],{i,1,Length[Ham2]}];
Alpha[J -I1-I2][J -I1]=Sum[Eigenvectors[Ham2][[4]]*FLIST[[i]],{i,1,Length[Ham2]}];
```

```
"This should rely diagonalize Ham2.Actually two very small (in the order 10^-16) off diagonal
   ellements remain, thats why the use of chop.";
Clear[Alist];Alist = {};
Do[Do[AppendTo[Alist, Alpha[F][Fi]], {F, Abs[Fi + I2], Abs[Fi - I2], -1}], {Fi, Abs[J + I1], Abs[J - I1], -1}]
Chop[Alist.Ham2.Transpose[Alist], 8] // MatrixForm // N
```

$$\begin{pmatrix} 747355. & 0. & 0. & 0. \\ 0. & 701526. & 0. & 0. \\ 0. & 0. & -1.18318 \times 10^{6} & 0. \\ 0. & 0. & 0. & -265702. \end{pmatrix}$$

"Now we construct the function that returns the energy as a function of F,a";

Clear[En];En[F_,a_]:=Alpha[F][a].Ham2.Alpha[F][a]

```
"And now we construct the eigenvectors C_{Fi,a}^(F) as defined in the above mentioned article, but
   labeled here as Eigenfunctions.";
Clear[Eigenfunction];
Eigenfunction[F_, Fi_, a_] := Fist[F][Fi].Alpha[F][a];

"And finally this is the depolarization function";
Clear[G];
G[k_, t_] :=
 Sum[
  ((2*F+1)*(2*Fp+1))/((2*I1+1)*(2*I2+1)) * Cos[2*Pi*(En[F, a]/(2F+1) - En[Fp, ap]/(2*Fp+1))*t] *
          (Sum[
                (-1)^(Fi+Fip) * Sqrt[(2*Fi+1)] * Sqrt[(2*Fip+1)] *
                 SixJSymbol[{Fip, J, I1}, {J, Fi, k}] * SixJSymbol[{Fip, Fp, I2}, {F, Fi, k}]
                 Eigenfunction[F, Fi, a] * Eigenfunction[Fp, Fip, ap]
                , {Fi, Abs[J+I1], Abs[J-I1], -1}
                , {Fip, Abs[J+I1], Abs[J-I1], -1}])^2
  , {a, Abs[J+I1], Abs[J-I1], -1}
  , {ap, Abs[J+I1], Abs[J-I1], -1}
  , {F, Abs[a+I2], Abs[a-I2], -1}
  , {Fp, Abs[ap+I2], Abs[ap-I2], -1}]


"This is G averaged";
Clear[Gav];
Gav[k_] :=
 Sum[
  (2*F+1)^2/((2*I1+1)*(2*I2+1)) *
          (Sum[
                (-1)^(Fi+Fip) * Sqrt[(2*Fi+1)] * Sqrt[(2*Fip+1)] *
                 SixJSymbol[{Fip, J, I1}, {J, Fi, k}] * SixJSymbol[{Fip, F, I2}, {F, Fi, k}]
                 Eigenfunction[F, Fi, a] * Eigenfunction[F, Fip, a]
                , {Fi, Abs[J+I1], Abs[J-I1], -1}
                , {Fip, Abs[J+I1], Abs[J-I1], -1}])^2
  , {a, Abs[J+I1], Abs[J-I1], -1}
  , {F, Abs[a+I2], Abs[a-I2], -1}
 ]

"Here we evaluate G average";
Gav[2]//N

 0.195452
```

```
"And here we plot G vs t";
Plot[Evaluate[G[2, x], {x, 0, 50 * 10^-6}], PlotRange → {-0.3, 1}, AxesOrigin → {0, -0.3}, PlotPoints → 80];
```

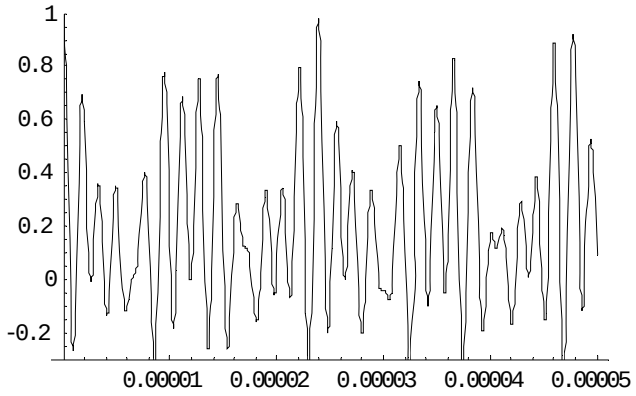


```
"And this is the polarization function";
Clear[Hf, Hh];
Hf[k_, t_] :=
 Sum[
  ((2 * F + 1) * (2 * Fp + 1)) / Sqrt[(2 * I1 + 1) * (2 * J + 1) * (2 * I2 + 1)] * Cos[2 * Pi * (En[F, a] / (2 F + 1) - En[Fp, ap] / (2 * Fp + 1)) * t] *
   (Sum[
     (-1)^(2 * Fip) * Sqrt[(2 * Fi + 1)] * Sqrt[(2 * Fip + 1)] *
      SixJSymbol[{Fi, Fip, k}, {Fp, F, I2}] * SixJSymbol[{Fi, Fip, k}, {I1, I1, J}]
      Eigenfunction[F, Fi, a] * Eigenfunction[Fp, Fip, ap]
     , {Fi, Abs[J + I1], Abs[J - I1], -1}
     , {Fip, Abs[J + I1], Abs[J - I1], -1}]) *
   (Sum[
     (-1)^(Fi + Fip) * Sqrt[(2 * Fi + 1)] * Sqrt[(2 * Fip + 1)] *
      SixJSymbol[{Fi, Fip, k}, {Fp, F, I2}] * SixJSymbol[{Fi, Fip, k}, {J, J, I1}]
      Eigenfunction[F, Fi, a] * Eigenfunction[Fp, Fip, ap]
     , {Fi, Abs[J + I1], Abs[J - I1], -1}
     , {Fip, Abs[J + I1], Abs[J - I1], -1}])
  , {a, Abs[J + I1], Abs[J - I1], -1}
  , {ap, Abs[J + I1], Abs[J - I1], -1}
  , {F, Abs[a + I2], Abs[a - I2], -1}
  , {Fp, Abs[ap + I2], Abs[ap - I2], -1}]
```

```
"Hf averaged with similar agruments";
Clear[Hfav];
Hfav[k_] :=
 Sum[
  (2*F+1)^2 / Sqrt[(2*I1+1)*(2*J+1)] * (2*I2+1) *
   (Sum[
     (-1)^(2*Fip) * Sqrt[(2*Fi+1)] * Sqrt[(2*Fip+1)] *
      SixJSymbol[{Fi, Fip, k}, {F, F, I2}] * SixJSymbol[{Fi, Fip, k}, {I1, I1, J}]
      Eigenfunction[F, Fi, a] * Eigenfunction[F, Fip, a]
     , {Fi, Abs[J+I1], Abs[J-I1], -1}
     , {Fip, Abs[J+I1], Abs[J-I1], -1}]) *
   (Sum[
     (-1)^(Fi+Fip) * Sqrt[(2*Fi+1)] * Sqrt[(2*Fip+1)] *
      SixJSymbol[{Fi, Fip, k}, {J, J, I1}] * SixJSymbol[{Fi, Fip, k}, {J, J, I1}]
      Eigenfunction[F, Fi, a] * Eigenfunction[F, Fip, a]
     , {Fi, Abs[J+I1], Abs[J-I1], -1}
     , {Fip, Abs[J+I1], Abs[J-I1], -1}])
  , {a, Abs[J+I1], Abs[J-I1], -1}
  , {F, Abs[a+I2], Abs[a-I2], -1}]


"All the evolutions ";


Plot[Evaluate[{G[1, x], Sqrt[(I1*(I1+1))/(J*(J+1))] * Hf[1, x], Sqrt[(I2*(I2+1))/(J*(J+1))] * Hh[1, x],
    G[1, x] + Sqrt[(I1*(I1+1))/(J*(J+1))] * Hf[1, x] + Sqrt[(I2*(I2+1))/(J*(J+1))] * Hh[1, x]}],
  {x, 0, 50*10^-6}, PlotRange -> {0, 1.1}, AxesOrigin -> {0, 0},
  PlotStyle -> {Hue[0.1], Hue[0.3], Hue[0.5], Hue[0.9]}, PlotPoints -> 50];
```

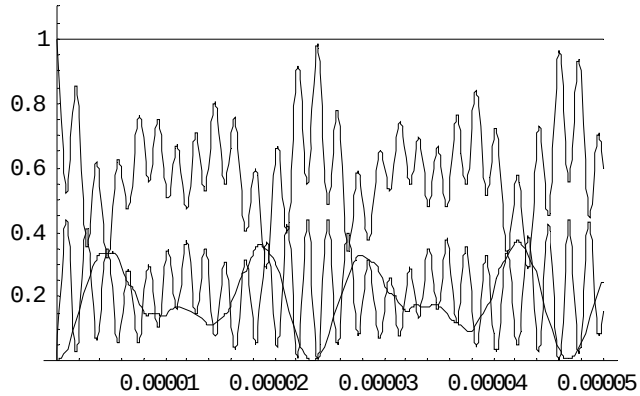

[1] R.J. Abraham, J. Fisher, and P. Loftus, *Introduction to NMR spectroscopy* (Wiley, New York, 1998).

[2] M. S. Albert, G. D. Cates, W. Happer, B. Saam, C. S. Springer, and A. Wishnia, *Nature* **370** 199 (1994).

[3] S. G. Resdun, R.J. Knize, G.D. Cates, and W. Happer, Phys. Rev. A **42**, 1293 (1990).

[4] E. Steffens, W. Haeberli, *Rep. Prog. Phys.* **66** 1887 (2003).

[5] C. T. Rettner, and R. N. Zare *J. Chem. Phys.* **77** 2416 (1982).

[6] P. R. Brooks, E. M. Jones, *J. Chem. Phys.* **45** 3449 (1966).

[7] R. N. Zare, *Science* **279** 1875 (1978)

[8] W. Gerlach, O. Stern, Ann. der Phys. **74**, 673 (1924).

[9] K. Zapfe, K. Braun, H.-G. Gaul, M. Griesner, B. Povh, M. Rall, E. Steffens, F. Stock, J. TonhOuser, C. Montag, F. Rathmann, D. Fick, W. Haeberli, *Rev. Sci. Instrum.* **66**, 28 (1995).

[10] W. Happer, *Rev. Mod. Phys.* **44**, 169 (1972).

[11] K.S.E. Eikema, J. Walz, and T.W. Hänsch, *Phys. Rev. Lett.* **83**, 3828 (1999)

[12] E. Babcock, I. Nelson, S. Kadlecek, B. Driehuys, L.W. Anderson, F.W. Hersman, T.G.Walker, *Phys. Rev.Lett.* **91**, 123003-1 (2003).

[13] S. Appelt, A. Ben-Amar Baranga, C. J. Erickson, M. V. Romalis, A. R. Young, W. Happer, *Phys.Rev. A*. **58**, 1412 (1998).

[14] R. J. van Brunt, R. N. Zare*, J. Chem. Phys.* **48**, 4304 (1968).

[15] A.J. Orr-Ewing, W.R. Simpson, T.P. Rakitzis, R.N. Zare, *Isr. J. Chem.* **34**, 95 (1994).

[16] Z.Karny, R.C.Estler and R.N.Zare J.Chem.Phys. **69** 11 (1978)

[17] Z.Karny and R.N.Zare J.Chem.Phys. **68** 8 (1978)

[18] C.H.Greene and R.N.Zare *Phys.Rev.A* **25** 4 (1982)

[19] R. Altkorn, R. N. Zare, C. H. Greene, *Mol. Phys.* **55** 1 (1985).

[20] J. Zhang, C. W. Riehn, M. Dulligan, C. Wittig, *J. Chem. Phys.* **104** 7027 (1996)

[21] T.P. Rakitzis et al., Science **300**, 1936 (2003).

[22] R. J. van Brunt, R. N. Zare, J. Chem. Phys. **48**, 4304 (1968).

[23] O.S. Vasyutinskii, Sov. Phys. JETP **54**, 855 (1981).

[24] R.N. Zare, *Angular Momentum* (Wiley, New York, 1988).

[25] A.J. Orr-Ewing, R.N. Zare, *Ann. Rev. Phys. Chem.* **45,** 315 (1994).

[26] I.I. Sobelman, *Introduction to the Theory of Atomic Spectra* (Pergamnon Press, 1972).

[27] U. Fano, G. Racah, *Irreducible Tensorial Sets* (Academic Press, 1959).

[28] M. Rutkowski, H. Zacharias, 301, 189 (2004).

[29] J. Zhang, C. W. Riehn, M. Dulligan, C. Wittig, *J. Chem. Phys.* **104** 7027 (1996).

[30] J. S. Muenter, W. Klemperer, *J. Chem. Phys.* **52,** 6033 (1970)

[31] E.W.Kaiser, J. Chem. Phys. **53**, 5 (1970)

[32] M.P.Docker Chemical Physics 135 (1989) 405-42 I

[33] S. Cureton-Chin, P.B. Kelly, M.P. Augustine, J. Chem. Phys. **116**, 4837 (2002).

[34] T.P. Rakitzis, ChemPhysChem **5**, 1489 (2004).

[35] A.M. Wodtke, Y.T. Lee, J. Phys. Chem. **89**, 4744 (1985).

[36] E.W.Kaiser, J. Chem. Phys. **53**, 5 (1970)

[37] H. Lammer, R.T. Carter, J.R. Huber, Eur. Phys. J. D **8**, 385 (2000).

[38] Gabriel G. Balint-Kurti, Alex Brown, Andrey G. Smolin and Oleg S. Vasyutinskii, *J. Phys. Chem. A,* **110** (16), 5371 -5378, (2006).

[39] Ch.Breant et al. Laser Spectroscopy 6 Springer-Verlag p138-143

[40] R.Weiss Phys. Rev.**131**, 2, 659 (1963).